

DOI:10.1002/ejic.201300364

## Functionalized Bis(pentafluoroethyl)phosphanes: Improved Syntheses and Molecular Structures in the Gas Phase

Alexander V. Zakharov,<sup>[a,b]</sup> Yury V. Vishnevskiy,<sup>[b]</sup> Nadine Allefeld,<sup>[c]</sup>  
Julia Bader,<sup>[c]</sup> Boris Kurscheid,<sup>[c]</sup> Simon Steinhauer,<sup>[c]</sup>  
Berthold Hoge,<sup>\*[c]</sup> Beate Neumann,<sup>[b]</sup> Hans-Georg Stammer,<sup>[b]</sup>  
Raphael J. F. Berger,<sup>[b][‡]</sup> and Norbert W. Mitzel<sup>\*[b]</sup>

*Dedicated to Professor Heinrich Nöth on the occasion of his 85th birthday*

**Keywords:** Phosphorus / Electron diffraction / Structure elucidation / Molecular dynamics / Density functional calculations / Fluorine

(C<sub>2</sub>F<sub>5</sub>)<sub>2</sub>PNEt<sub>2</sub> represents an excellent starting material for the selective synthesis of bis(pentafluoroethyl)phosphane derivatives. The moderately air-sensitive aminophosphane is accessible on a multi-gram scale by treating Cl<sub>2</sub>PNEt<sub>2</sub> with C<sub>2</sub>F<sub>5</sub>Li. Treatment with gaseous HCl or HBr yielded the corresponding phosphane halides (C<sub>2</sub>F<sub>5</sub>)<sub>2</sub>PCl and the so far unknown (C<sub>2</sub>F<sub>5</sub>)<sub>2</sub>PBr in good yields. The hitherto unknown (C<sub>2</sub>F<sub>5</sub>)<sub>2</sub>PF was obtained by treating (C<sub>2</sub>F<sub>5</sub>)<sub>2</sub>PBr with excess antimony trifluoride. Treatment of (C<sub>2</sub>F<sub>5</sub>)<sub>2</sub>PCl with Bu<sub>3</sub>SnH led to the quantitative formation of (C<sub>2</sub>F<sub>5</sub>)<sub>2</sub>PH. Deprotonation formally yielded the (C<sub>2</sub>F<sub>5</sub>)<sub>2</sub>P<sup>-</sup> anion in a form that was stabilized by coordination to mercury ions to form the complex [Hg{P(C<sub>2</sub>F<sub>5</sub>)<sub>2</sub>}<sub>2</sub>(dppe)]. An improved high-yielding synthesis of (C<sub>2</sub>F<sub>5</sub>)<sub>2</sub>POH was achieved by treating (C<sub>2</sub>F<sub>5</sub>)<sub>2</sub>PNEt<sub>2</sub> with *p*-toluenesulfonic acid. The gas-phase structures of (C<sub>2</sub>F<sub>5</sub>)<sub>2</sub>PH and (C<sub>2</sub>F<sub>5</sub>)<sub>2</sub>POH were determined by electron diffraction. The vibrational corrections employed in the data analysis of the diffraction data were derived from molecular dynamics

calculations. Both compounds exist in the gas phase mostly as C<sub>1</sub>-symmetric *cis,cis* conformers with regard the orientation of the C<sub>2</sub>F<sub>5</sub> groups relative to the functional groups H and OH. The presence of a second conformer at ambient temperature is likely in both cases. The refined amounts of dominant conformers are 94(6) and 85(6) % for (C<sub>2</sub>F<sub>5</sub>)<sub>2</sub>PH and (C<sub>2</sub>F<sub>5</sub>)<sub>2</sub>POH, respectively. The conformational behaviour was further explored by potential energy surface scans based on DFT calculations. Important experimental structural parameters for the most stable conformers are  $r_e(\text{P-C})_{\text{average}} = 1.884(3)$  Å for (C<sub>2</sub>F<sub>5</sub>)<sub>2</sub>PH and  $r_e(\text{P-C})_{\text{average}} = 1.894(4)$  Å and  $r_e(\text{P-O}) = 1.582(3)$  Å for (C<sub>2</sub>F<sub>5</sub>)<sub>2</sub>POH. The different coordination properties of (C<sub>2</sub>F<sub>5</sub>)<sub>3</sub>P, (C<sub>2</sub>F<sub>5</sub>)<sub>2</sub>POH, (CF<sub>3</sub>)<sub>3</sub>P and (CF<sub>3</sub>)<sub>2</sub>POH were evaluated by complex formation with [Ni(CO)<sub>4</sub>]: the maximum achievable number of CO ligands substituted by (C<sub>2</sub>F<sub>5</sub>)<sub>3</sub>P is 1, by (C<sub>2</sub>F<sub>5</sub>)<sub>2</sub>POH is 2, by (CF<sub>3</sub>)<sub>3</sub>P is 3 and by the smallest ligand (CF<sub>3</sub>)<sub>2</sub>POH is 4.

### Introduction

Phosphane ligands are essential for the synthesis of metal complexes used in a variety of catalytic reactions.<sup>[1]</sup> Com-

pared with the vast number of  $\pi$ -donating phosphanes,  $\pi$ -accepting ligands are relatively uncommon. One of the most electron-deficient and  $\pi$ -acidic phosphane derivatives is P(CF<sub>3</sub>)<sub>3</sub>.<sup>[2]</sup> It is highly volatile and air-sensitive and hence unsuitable for technical applications. By comparison, the next highest homologue, the less volatile P(C<sub>2</sub>F<sub>5</sub>)<sub>3</sub>, can be handled by using common Schlenk techniques. However, the high steric demand of the pentafluoroethyl groups prevents P(C<sub>2</sub>F<sub>5</sub>)<sub>3</sub> from being employed as a ligand in coordination chemistry and not a single complex is known. P(C<sub>2</sub>F<sub>5</sub>)<sub>3</sub> in the solid state and gas phase has a Tolman cone angle of 193 and 191°, respectively;<sup>[3]</sup> the conformational behaviour of the C<sub>2</sub>F<sub>5</sub> substituents in P(C<sub>2</sub>F<sub>5</sub>)<sub>3</sub> depends on repulsive F...F contacts.<sup>[3]</sup>

Substitution of one pentafluoroethyl group by a sterically less demanding substituent leads to more complicated conformational behaviour, as has been demonstrated for (C<sub>2</sub>F<sub>5</sub>)<sub>2</sub>PCl, which has also been studied by gas electron diffraction

- [a] Ivanovo State University of Chemistry and Technology, Department of Physics, Engels Av. 7, 153000 Ivanovo, Russia  
[b] Fakultät für Chemie, Lehrstuhl für Anorganische Chemie und Strukturchemie, Universität Bielefeld, Universitätsstraße 25, 33615 Bielefeld, Germany  
E-mail: mitzel@uni-bielefeld.de  
Homepage: www.uni-bielefeld.de/chemie/arbeitsbereiche/ac3-mitzel  
[c] Fakultät für Chemie, Anorganische Chemie II, Universität Bielefeld, Universitätsstraße 25, 33615 Bielefeld, Germany  
E-mail: b.hoge@uni-bielefeld.de  
Homepage: www.uni-bielefeld.de/chemie/acii/hoge  
[‡] Present address: FB Materialwissenschaften und Physik, Paris-Lodron Universität Salzburg, Hellbrunner Str. 34, 5020 Salzburg, Austria  
Supporting information for this article is available on the WWW under <http://dx.doi.org/10.1002/ejic.201300364>.

(GED).<sup>[4]</sup> Such compounds with sterically more accessible phosphorus atoms allow manifold coordination chemistry. A prominent example of this is the chelating ligand  $(C_2F_5)_2PC_2H_4P(C_2F_5)_2$  with two  $P(C_2F_5)_2$  groups. It forms the basis for a diverse range of complexes, many of which exhibit promising catalytic activities.<sup>[5]</sup>

$(C_2F_5)_2PC_2H_4P(C_2F_5)_2$  was first synthesized by Ernst and Roddick in 1989 by the reaction of  $LiC_2F_5$  with  $Cl_2PC_2H_4PCl_2$ .<sup>[6]</sup> In contrast to  $LiCF_3$ , which eliminates lithium fluoride even at temperatures below  $-100\text{ }^\circ\text{C}$ ,<sup>[7]</sup>  $LiC_2F_5$  is stable up to  $-50\text{ }^\circ\text{C}$ .<sup>[8]</sup> It can be generated in situ by treating  $C_2F_5Cl$  or  $C_2F_5H$  with  $nBuLi$  in diethyl ether.<sup>[6,9]</sup> The  $C_2F_5$  group can also be introduced by the fluoride-mediated reaction of  $C_2F_5SiMe_3$  with  $(PhO)_2PC_2H_4P(OPh)_2$ .<sup>[10]</sup>

The reaction of white phosphorus with  $C_2F_5I$  under high pressure and temperatures is not a favourable alternative to the synthesis of bis(pentafluoroethyl)phosphane derivatives. Mono- and bis(pentafluoroethyl)iodophosphane were obtained in this way only in very low yields.<sup>[11]</sup> Treating the iodo compounds with silver or mercury chloride furnishes the corresponding chloro derivatives.<sup>[12]</sup> Recently published, significantly improved syntheses of  $(C_2F_5)_2PCl$ <sup>[4]</sup> and  $(C_2F_5)_2POH$ <sup>[13]</sup> start from the technical product  $(C_2F_5)_3PF_2$  and proceed via  $P(C_2F_5)_3$  and  $(C_2F_5)_2PO^-$  salts as intermediates, respectively. The improved protocol for the synthesis of  $(C_2F_5)_2POH$  has allowed the preparation of several stable and catalytically active transition-metal complexes.<sup>[13]</sup>  $(C_2F_5)_2PH$  is formed as a side-product in the synthesis of  $P(C_2F_5)_3$  by reduction of  $(C_2F_5)_3PF_2$  with  $NaBH_4$ .<sup>[14]</sup>

$(CF_3)_2PNEt_2$  has been shown to represent an ideal starting material for the synthesis of (trifluoromethyl)phosphane derivatives.<sup>[15]</sup> It is accessible on a multi-gram scale by the Ruppert procedure<sup>[16]</sup> and is only slightly air-sensitive. The aminophosphane  $(CF_3)_2PNEt_2$  can be transformed by gaseous  $HBr$  into  $(CF_3)_2PBr$  and the bis(trifluoromethyl)phosphinous acid,  $(CF_3)_2POH$ , can be obtained by treating  $(CF_3)_2PNEt_2$  with excess *p*-toluenesulfonic acid.

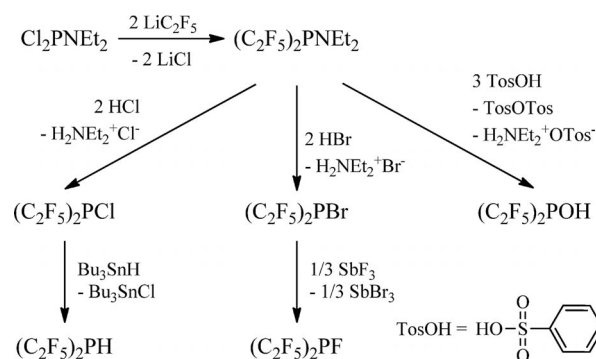
In analogy, the known aminophosphane  $(C_2F_5)_2PNEt_2$  has shown promise as a starting material for the synthesis of new functional bis(pentafluoroethyl)phosphane derivatives  $(C_2F_5)_2PX$  ( $X = F, Br$ ) and selective access to known compounds ( $X = H, Cl, OH$ ). In this contribution we demonstrate such improved preparative protocols as well as a detailed analysis of the gas-phase structures of  $(C_2F_5)_2POH$  and  $(C_2F_5)_2PH$ .

## Results and Discussion

### Preparation of Bis(pentafluoroethyl)phosphane Derivatives

Previous work has shown that  $LiC_2F_5$  is well suited to the efficient pentafluoroethylation of chlorophosphane derivatives by nucleophilic substitution.<sup>[17]</sup> It was generated in situ according to a literature method<sup>[9]</sup> and subsequently treated with  $Cl_2PNEt_2$ . The product,  $(C_2F_5)_2PNEt_2$ , was isolated by vacuum distillation as a colourless liquid.

Exposure of neat  $(C_2F_5)_2PNEt_2$  to gaseous hydrogen chloride led to P–N bond cleavage and quantitative formation of  $(C_2F_5)_2PCl$  (Scheme 1). Completion of the reaction was monitored by evaporating all the volatile components followed by further treatment with gaseous  $HCl$  until no further precipitation of ammonium salts was observed. After removal of excess  $HCl$ , the resulting colourless liquid was identified as  $(C_2F_5)_2PCl$  by multi-nuclear NMR<sup>[18]</sup> and IR spectroscopy.<sup>[12]</sup>



Scheme 1. Reaction pathways for the syntheses of bis(pentafluoroethyl)phosphane derivatives  $(C_2F_5)_2PX$  ( $X = H, F, Cl, Br, OH$ ).

The bromo derivative  $(C_2F_5)_2PBr$  was synthesized analogously by treating  $(C_2F_5)_2PNEt_2$  with gaseous hydrogen bromide. The yield of the colourless liquid  $(C_2F_5)_2PBr$  was 70% (Scheme 1). The  $^{19}F$  NMR spectrum exhibits a signal for the  $CF_3$  unit at  $\delta = -80.6$  ppm and a multiplet of higher order for the  $CF_2$  unit at  $\delta = -112.0/-114.1$  ppm. The higher-order pattern is due to the diastereotopic nature of the fluorine atoms of the  $CF_2$  unit.

In contrast, gaseous hydrogen fluoride cannot be used to generate the corresponding fluorophosphane from  $(C_2F_5)_2PNEt_2$ . The results of this reaction will be published elsewhere. We employed antimony trifluoride as an alternative, a reagent with known potential for transformation of halophosphane derivatives into the corresponding fluorophosphanes.<sup>[19]</sup> Treatment of  $(C_2F_5)_2PBr$  with  $SbF_3$  at ambient temperature led to the selective formation of the so far unknown  $(C_2F_5)_2PF$  as a colourless liquid within two days (Scheme 1). In contrast, the reaction of  $(C_2F_5)_2PCl$  with  $SbF_3$  remained incomplete even after seven days at ambient temperature. The  $^{19}F$  NMR spectrum of  $(C_2F_5)_2PF$  reflects the chemically and magnetically non-equivalent fluorine atoms. A resonance arising from the  $CF_3$  group is observed at  $\delta = -82.4$  ppm with  $^3J(F,F)$  coupling between the  $CF_3$  group and the fluorine atom directly attached to the phosphorus atom. The resonance of the diastereotopic  $CF_2$  group is a high-order pattern. The resonance of the fluorine atom directly bound to the phosphorus atom is split by the characteristic  $^1J(P,F)$  coupling of 1015 Hz ( $\delta = -216.7$  ppm) into a pattern that can be completely described as an  $[AB]_2M_6GX$  ( $A, B, G, M = F; X = P$ ) spin system. For comparison, Table 1 compiles a set of NMR parameters for compounds containing  $(C_2F_5)_2P$  units.

Table 1. Selected  $^{31}\text{P}$  and  $^{19}\text{F}$  NMR spectroscopic data for bis(pentafluoroethyl)phosphane derivatives.<sup>[a]</sup>

	$\delta(^{31}\text{P})$ [ppm]	$^3J(\text{P},\text{F})$ [Hz]	$\delta(^{19}\text{CF}_3)$ [ppm]	$\delta(^{19}\text{CF}_a\text{F}_b)$ [ppm]	$\delta(^{19}\text{CF}_a\text{F}_b)$ [ppm]
$(\text{C}_2\text{F}_5)_2\text{PNEt}_2$ <sup>[b]</sup>	46.8	–	–82.1	–116.1	117.0
$(\text{C}_2\text{F}_5)_2\text{PBr}$	44.0	17	–80.6	–112.0	–114.1
$(\text{C}_2\text{F}_5)_2\text{PCl}$	62.2	16	–80.2	–	–115.9 <sup>[c]</sup>
$(\text{C}_2\text{F}_5)_2\text{PF}$ <sup>[d,e]</sup>	137.6	13	–82.4	–123.7	–125.0
$(\text{C}_2\text{F}_5)_2\text{PH}$ <sup>[f]</sup>	–50.8	13	–84.8	–103.0	–109.0
$(\text{C}_2\text{F}_5)_2\text{POH}$	93.0	18	–82.1	–123.4	–125.4

[a] Data measured in  $[\text{D}_6]\text{acetone}$ . [b] Determined in  $\text{CDCl}_3$ . [c] Fluorine atoms in the  $\text{CF}_2$  group are equivalent. [d]  $\delta(^{31}\text{P}) = 137.6$  ppm [m, d,  $^1J(\text{P},\text{F}) = 1015$  Hz]. [e]  $\delta(^{19}\text{F}) = -216.7$  ppm [d,  $^1J(\text{P},\text{F}) = 1015$  Hz,  $(\text{C}_2\text{F}_5)_2\text{PF}$ ]. [f]  $\delta(^{31}\text{P}) = -50.8$  ppm [m, d,  $^1J(\text{P},\text{H}) = 231$  Hz],  $^3J(\text{P},\text{F}) = 18$  Hz.

The P–N bond could also be cleaved by treatment with sulfonic acids.<sup>[15]</sup> The reaction of  $(\text{C}_2\text{F}_5)_2\text{PNEt}_2$  with at least 5 equivalents of dried *p*-toluenesulfonic acid in the less volatile solvent 1,6-dibromohexane led to a quantitative conversion to  $(\text{C}_2\text{F}_5)_2\text{POH}$  (Scheme 1). The phosphinous acid is the only volatile compound and was isolated by fractional condensation in yields better than 90%. The experimental NMR spectroscopic data are in good agreement with literature data.<sup>[13]</sup>

Bis(pentafluoroethyl)phosphane,  $(\text{C}_2\text{F}_5)_2\text{PH}$ , was easily accessed from bis(pentafluoroethyl)halophosphanes by treatment with  $\text{Bu}_3\text{SnH}$  (Scheme 1). After the reaction of neat  $(\text{C}_2\text{F}_5)_2\text{PCl}$  with a slight excess of  $\text{Bu}_3\text{SnH}$  at room temperature, pure  $(\text{C}_2\text{F}_5)_2\text{PH}$  was isolated by fractional condensation in quantitative yield. The NMR spectroscopic data are in agreement with the literature.<sup>[13]</sup> IR spectroscopic investigations revealed the P–H stretching mode at  $2349\text{ cm}^{-1}$ .

Deprotonation of  $(\text{C}_2\text{F}_5)_2\text{PH}$  with  $[\text{Hg}(\text{CN})_2\text{dppe}]$  led to the formation of the bis(pentafluoroethyl)phosphanide anion,  $(\text{C}_2\text{F}_5)_2\text{P}^-$ , stabilized by coordination to the mercury cation. The reaction proceeded via the monosubstituted mercury complex  $[\text{Hg}(\text{CN})\{\text{P}(\text{C}_2\text{F}_5)_2\}(\text{dppe})]$  to give the final product  $[\text{Hg}\{\text{P}(\text{C}_2\text{F}_5)_2\}_2(\text{dppe})]$ . The intermediate was characterized by NMR spectroscopy [ $^1J(\text{Hg},\text{P}) = 1289$  Hz] and crystallography (see Figure 1, which also lists structural parameters in the caption). The NMR properties of  $[\text{Hg}\{\text{P}(\text{C}_2\text{F}_5)_2\}_2(\text{dppe})]$  are comparable to those of its  $\text{CF}_3$  analogue.<sup>[20]</sup> The  $^{31}\text{P}\{^{19}\text{F}\}$  NMR spectrum exhibits, in addition to a signal for the dppe ligand [ $\delta(^{31}\text{P}) = 11.2$  ppm], a triplet at  $\delta = -9.2$  ppm with a  $^2J(\text{P},\text{P})$  coupling constant of 58 Hz and  $^{199}\text{Hg}$  satellites [ $^1J(\text{Hg},\text{P}) = 824$  Hz]. Consequently, the resonance in the  $^{199}\text{Hg}$  NMR spectrum at  $\delta = 296.2$  ppm is a triplet of triplets due to its coupling to different phosphorus atoms.

Recrystallization from toluene yielded single crystals of  $[\text{Hg}\{\text{P}(\text{C}_2\text{F}_5)_2\}_2(\text{dppe})]\cdot\text{C}_7\text{H}_8$  suitable for X-ray diffraction. The complex crystallizes in the monoclinic space group  $Pc$ . The molecular structure of the complex, shown in Figure 2, is similar to that of the  $\text{CF}_3$  analogue.<sup>[20]</sup> The mercury atom exhibits a strongly distorted tetrahedral coordination

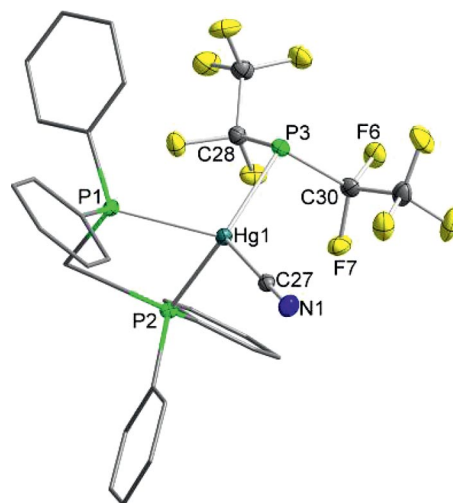


Figure 1. Molecular structure of  $[\text{Hg}\{\text{P}(\text{C}_2\text{F}_5)_2\}(\text{CN})(\text{dppe})]$  in the solid state. Hydrogen atoms and toluene as solvent molecule have been omitted for clarity. Relevant atoms are shown as displacement ellipsoids at the 50% probability level. Selected bond lengths [ $\text{\AA}$ ] and angles [ $^\circ$ ]: Hg1–P1 2.615(1), Hg1–P2 2.565(1), Hg1–P3 2.490(1), Hg1–C27 2.178(3), C27–N1 1.132(3), P3–C28 1.893(3), P3–C30 1.884(3), P1–Hg1–P2 82.0(1), P3–Hg1–C27 116.6(1), P1–Hg1–P3 111.9(1), P2–Hg1–C27 113.7(1).

sphere with a  $(\text{C}_2\text{F}_5)_2\text{P–Hg–P}(\text{C}_2\text{F}_5)_2$  angle of  $123.7(1)^\circ$  and a  $\text{Ph}_2\text{P–Hg–PPh}_2$  angle of  $80.4(1)^\circ$ . Possible effects of negative hyperconjugation are evident in the elongated C–F distances, the mean for the  $\text{CF}_2$  units being  $1.36\text{ \AA}$ , which compares with a similarly long average of  $1.345\text{ \AA}$  in the gaseous state of the neutral compound  $(\text{C}_2\text{F}_5)_2\text{PH}$ .

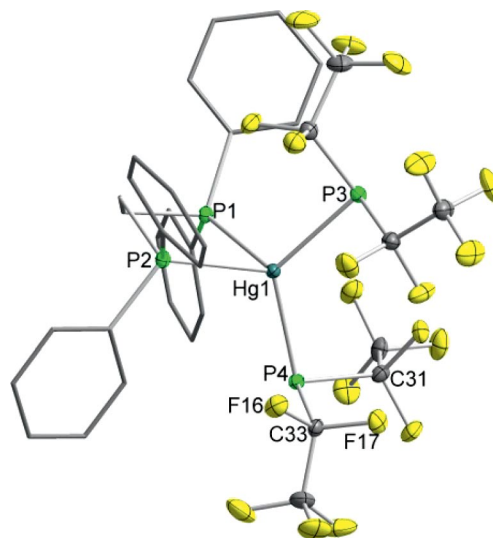


Figure 2. Molecular structure of  $[\text{Hg}\{\text{P}(\text{C}_2\text{F}_5)_2\}_2(\text{dppe})]\cdot\text{C}_7\text{H}_8$  in the solid state. Hydrogen atoms and toluene as the solvent molecule have been omitted for clarity. Relevant atoms are shown as displacement ellipsoids at the 50% probability level. Selected bond lengths [ $\text{\AA}$ ] and angles [ $^\circ$ ]: Hg1–P1 2.686(1), Hg1–P2 2.580(1), Hg1–P3 2.507(1), Hg1–P4 2.505(1), P4–C31 1.882(3), P4–C33 1.885(3), P1–Hg1–P2 80.4(1), P3–Hg1–P4 123.7(1), P1–Hg1–P3 108.6(1), P2–Hg1–P4 114.8(1).

## Gas-Phase Structures

The thermally averaged molecular structures determined by experimental gas-phase electron diffraction (GED) represent the weighted (Boltzmann) averages over all the vibrational states. As a consequence, they are geometrically inconsistent (i.e., internuclear distances cannot be used to construct a consistent model of Cartesian coordinates); this is also called the “shrinkage effect”,<sup>[21,22]</sup> which can be accounted for by applying vibrational corrections to the equilibrium internuclear distances, which improves the quality of refined experimental parameters. This also allows a more accurate comparison between quantum chemically calculated and experimentally determined structures. There are a number of approaches for the computation of these corrections. These include the “rectilinear harmonic approximation”<sup>[23,24]</sup> (implemented, for example, in the programs ASYM40<sup>[23,24]</sup> and SHRINK;<sup>[25–28]</sup> first approximation:  $k_{h0}$ ), the improved “curvilinear harmonic approximation”<sup>[26,28]</sup> (implemented in SHRINK; second approximation:  $k_{h1}$ ) and the more realistic “anharmonic approximation” (also implemented in SHRINK;  $k_3$ , calculated at the first-order perturbation theory level by using third derivatives of the potential energy<sup>[28]</sup>). A novel approach involves calculating vibrational corrections by using molecular dynamics (MD).<sup>[29,30]</sup> The last two methods were applied in the two structure determinations in this contribution, and the MD method has been further developed in this context.

### $(C_2F_5)_2PH$

The  $(C_2F_5)_2PH$  molecule has two enantiomers separated by a very small ( $0.25 \text{ kJ mol}^{-1}$ , B3LYP/cc-pVTZ calculation) barrier to inversion corresponding to a saddle-point structure of  $C_s$  symmetry with an imaginary frequency of  $14 \text{ cm}^{-1}$  (B3LYP/cc-pVTZ). However, enantiomers cannot be distinguished by GED. Consequently, data analysis was carried out for only one of them.

According to the potential energy surface (PES) analysis (Figure 3), there are six conformers of  $(C_2F_5)_2PH$  for each enantiomer. Table 2 shows the O3LYP/aug-cc-pVTZ energies and abundances of the conformers; B3LYP/cc-pVTZ data are provided in the Supporting Information. Most of the conformers are structurally similar to those of  $(C_2F_5)_2PCl$ ,<sup>[4]</sup> the difference being that there is only one minimum for conformer **II** of  $(C_2F_5)_2PH$  instead of two very close lying minima on the PES for  $(C_2F_5)_2PCl$  (conformers **2** and **3** in the notation in ref.<sup>[4]</sup>). Hence, theory predicts two major conformers for  $(C_2F_5)_2PH$  whereas all the others have higher energies and abundances that are too low at the temperature of the GED study to be reliably detectable. Consequently, the data analysis was restricted to the two lowest-energy conformers **I** and **II** shown in Figure 4.

We undertook molecular dynamics (MD) simulations and it was interesting to note that conformer **II** was present in 18% of the steps in these simulations starting from the equilibrium structure of the first conformer. Therefore MD simulations may also be used to estimate the conformational composition.

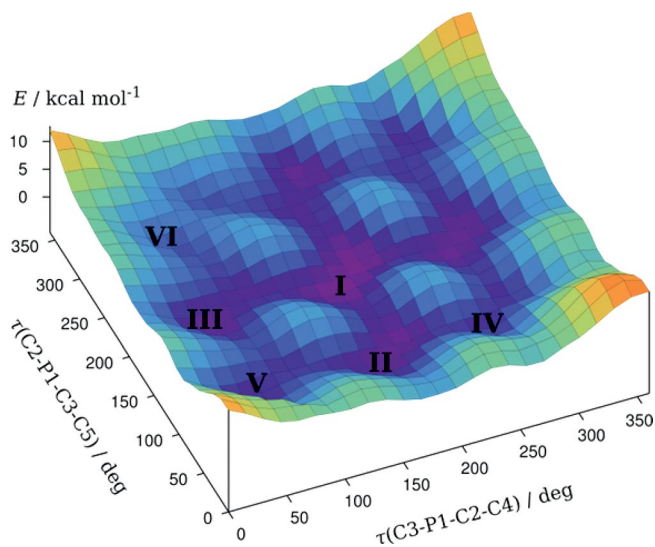


Figure 3. Potential energy surface diagram of  $(C_2F_5)_2PH$  for rotation around two P–C bonds [ $\tau(C3-P1-C2-C4)$  and  $\tau(C2-P1-C3-C5)$  dihedral angles] calculated at the B3LYP/6-31++G(d,p) level of theory.

Table 2. Conformers of  $(C_2F_5)_2PH$ , their torsion angles, relative energies and abundances at 295.15 K calculated at the O3LYP/aug-cc-pVTZ level of theory.

Conf.	$\tau(C2-P1-C3-C5)$ [°]	$\tau(C3-P1-C2-C4)$ [°]	$\Delta E$ [kcal mol <sup>-1</sup> ]	$\Delta G^\circ$ [kcal mol <sup>-1</sup> ]	$x$ [mol-%]
<b>I</b>	173.4	163.7	0.00	0.00	61.6
<b>II</b>	76.5	155.5	0.52	0.61	21.9
<b>III</b>	170.5	51.0	0.62	1.10	9.6
<b>IV</b>	81.5	-113.0	1.28	1.85	2.7
<b>V</b>	77.9	46.2	1.26	2.00	2.1
<b>VI</b>	-108.8	66.8	2.07	2.00	2.1

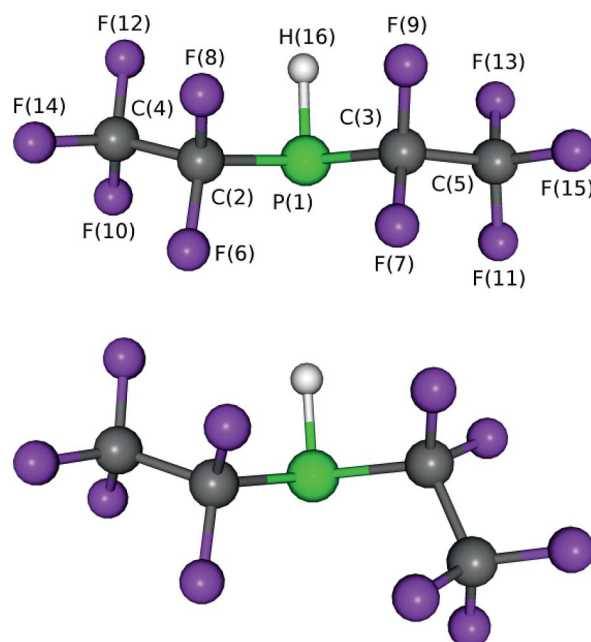


Figure 4. Calculated molecular structures of the two major conformers of  $(C_2F_5)_2PH$ , **I** (upper) and **II** (lower).

The refinement of GED data by using MD corrections for the vibrational parameters yielded the lowest disagreement factor ( $R_f = 4.6\%$ ), but differences between the structural parameters obtained from refinements performed by using the  $k_{h1}$  and  $k_3$  corrections were negligibly small. Inclusion of conformer **II** in the amount calculated (22 mol-%) did not lead to significant changes in the  $R_f$  factor. However, inclusion of conformer **II** in amounts larger than 25% led to a significant (by the Fisher criterion) increase in the  $R_f$  factor and a model consisting solely of conformer **II** produced a very high  $R_f$  factor (9.4%). Refinement by varying the conformer ratio (starting with 80% of conformer **I**) resulted in 94(6)% abundance of the first conformer with its structural parameters being very similar to those found by refinement of the single-conformer model. Therefore we can conclude that conformer **I** is dominant, with an abundance larger than 75%, although the ratio determined from the GED data has rather limited accuracy. The difference in the energies yielded by DFT computations is probably underestimated (as it appears to rise with increasing level of theory) and the actual abundance of conformer **II** is lower than predicted by calculations.

The major structural parameters of  $(C_2F_5)_2PH$  obtained from the GED experiment (single conformer model) by using  $k_3$  and MD sets of vibrational corrections, as well as from computations, are presented in Table 3 (the parameters obtained by using  $k_{h1}$  corrections are available in the Supporting Information for comparison). The radial distribution  $f(r)$  curve is presented in Figure 5 and the molecular intensity  $sM(s)$  curves are provided in the Supporting Information.

The bond lengths calculated by using the B3LYP functional paired with the cc-pVTZ basis set for P, C and H and aug-cc-pVTZ for F are generally overestimated. The calculated C–C and P–C distances are of poor quality, especially when comparing them with experimental  $r_e$  (not  $r_{h1}$ ) values. In better agreement with the experiment are the bond lengths computed at the O3LYP/aug-cc-pVTZ level of theory. The C–F distances are especially remarkable, as their differences are within experimental error, but the calculated C–C and P–C distances still show rather poor agreement with experimental values. Calculations at the MP2/aug-cc-pVTZ level produced values for  $r_e(P-C)$  in agreement with experiment; all F–C distances in this computation are very slightly elongated (by ca. 0.005 Å); the C–C bond length is still too large (by 0.011–0.012 Å), but the agreement is much better than in the case of DFT calculations. This halogen-rich compound appears to be a difficult case for quantum chemistry because none of the applied levels of theory was able to reproduce the experimental geometry with an accuracy better than 0.01 Å for all bond lengths.

We can compare the bond lengths with those of the  $(C_2F_5)_2PCL$  molecule studied previously by GED.<sup>[4]</sup> In that study a two-conformer model was applied and the second most abundant conformer was detectable; the abundance of the major conformer was 61(5)%. These first and second conformers of  $(C_2F_5)_2PCL$  are similar to those of  $(C_2F_5)_2PH$ , but, because the abundance of the second conformer in our experiment was small and could not be detected with sufficient accuracy, we compare the parameters of the first (major) conformer only. Corrections of  $k_{h1}$  type were used

Table 3. Major geometrical parameters for conformer **I** in the  $(C_2F_5)_2PH$  molecule.<sup>[a]</sup>

	$r_e$ ( $k_3$ ) <sup>[b]</sup>	GED		B3LYP/cc-pVTZ	O3LYP/aug-cc-pVTZ	MP2/aug-cc-pVTZ
		$r_g$ ( $k_{MD}$ ) <sup>[c]</sup>	$r_e$ ( $k_{MD}$ ) <sup>[c]</sup>	$r_e$	$r_e$	$r_e$
$r(P1-C2)$	1.876(3)	1.897(3)	1.882(3)	1.916	1.900	1.881
$r(P1-C3)$	1.880(3)	1.896(3)	1.886(3)	1.920	1.905	1.886
$r(C2-C4)$	1.516(3)	1.533(3)	1.519(3)	1.555	1.549	1.531
$r(C3-C5)$	1.515(3)	1.535(3)	1.518(3)	1.554	1.547	1.529
$r(C2-F6)$	1.344(1)	1.349(1)	1.346(1)	1.359	1.347	1.352
$r(C2-F8)$	1.341(1)	1.348(1)	1.343(1)	1.355	1.343	1.349
$r(C3-F7)$	1.343(1)	1.349(1)	1.344(1)	1.357	1.345	1.350
$r(C3-F9)$	1.341(1)	1.348(1)	1.343(1)	1.355	1.343	1.348
$r(C4-F10)$	1.325(1)	1.333(1)	1.328(1)	1.340	1.329	1.332
$r(C4-F12)$	1.327(1)	1.337(1)	1.330(1)	1.342	1.331	1.333
$r(C4-F14)$	1.318(1)	1.327(1)	1.322(1)	1.332	1.323	1.324
$r(C5-F11)$	1.323(1)	1.332(1)	1.326(1)	1.337	1.327	1.328
$r(C5-F13)$	1.330(1)	1.336(1)	1.333(1)	1.344	1.334	1.336
$r(C5-F15)$	1.318(1)	1.327(1)	1.323(1)	1.332	1.323	1.324
$\alpha(C2-P1-C3)$	98.6(6)		98.4(8)	97.4	97.4	95.1
$\alpha(C4-C2-P1)$	111.3(2)		112.6(2)	111.7	111.2	111.2
$\alpha(C5-C3-P1)$	110.4(2)		111.7(2)	110.8	110.2	110.2
$\tau(C4-C2-C1-C3)$	133(2)		166(3)	162.8	162.4	159.9
$\tau(C5-C3-P1-C2)$	143(2)		176(3)	173.2	172.8	168.4
$R_f$ [%]	4.7	4.6				

[a] The uncertainties quoted in parentheses are  $3\sigma_{LS}$ . Bond lengths of the same kind (P–C, C–C and C–F) were refined in groups  $g1-g3$  with fixed differences (see the Exp. Sect. for details) and therefore the  $3\sigma_{LS}$  uncertainties represent least-squares analysis errors of these groups, not individual bond lengths. Distances are given in Å and angles in degrees. [b] Fixed differences from B3LYP/cc-pVTZ calculations. [c] Fixed differences from O3LYP/aug-cc-pVTZ calculations.

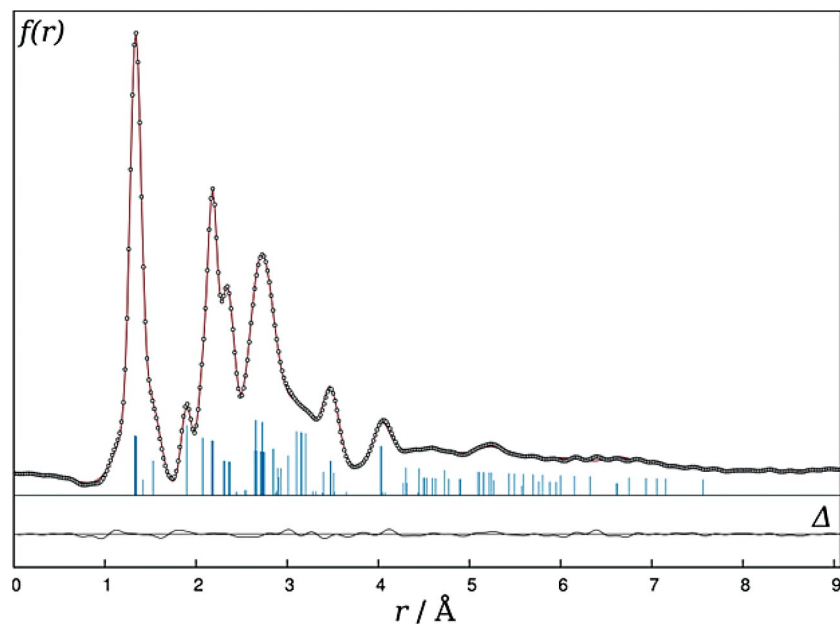


Figure 5. Experimental (dots) and theoretical (line) radial distribution  $f(r)$  curves and the difference curve (below) for  $(\text{C}_2\text{F}_5)_2\text{PH}$ . Vertical bars indicate the interatomic distances.

in the study of  $(\text{C}_2\text{F}_5)_2\text{PCl}$ ,<sup>[4]</sup> so  $r_g$  distances from our refinement, which also used  $k_{h1}$  corrections, are compared. The  $r_g(\text{P}-\text{C})$  distances in  $(\text{C}_2\text{F}_5)_2\text{PH}$  [1.897(3) and 1.896(3) Å] are comparable to those in  $(\text{C}_2\text{F}_5)_2\text{PCl}$  [1.904(3) and 1.894(3) Å]. The average  $r_g(\text{C}-\text{F}) = 1.351(1)$  Å for  $\text{CF}_2$  and  $r_g(\text{C}-\text{F}) = 1.332(1)$  Å for  $\text{CF}_3$ , which are the same as those in  $(\text{C}_2\text{F}_5)_2\text{PCl}$  within experimental error.

Note that the  $3\sigma_{\text{LS}}$  uncertainties given in Table 3 represent only least-squares errors. Because the geometrical parameters were refined in groups with fixed differences, these errors represent uncertainties in the groups, not for individual bond lengths. Moreover, there are uncertainties in the differences, because their values vary between levels of theory. Although the differences in the  $r(\text{P}-\text{C})$  and  $r(\text{C}-\text{C})$  bond lengths yielded by the B3LYP/cc-pVTZ, O3LYP/aug-cc-pVTZ and MP2/aug-cc-pVTZ calculations agree to within 0.001 Å, the differences in  $r(\text{C}-\text{F})$  often vary by 0.002–0.004 Å. Therefore the total errors for  $r(\text{C}-\text{F})$  may be several times larger than the  $3\sigma_{\text{LS}}$  uncertainty.

It is also interesting to compare the anharmonic vibrational corrections computed by two approaches, namely by molecular dynamics<sup>[29,30]</sup> and the SHRINK procedure,<sup>[31]</sup> by using potential energy third derivatives. The corrections ( $k = r_a - r_e$ ) for all the bonded distances in  $(\text{C}_2\text{F}_5)_2\text{PH}$  calculated by these two methods are available in the Supporting Information. Corrections to  $r(\text{P}-\text{C})$  and  $r(\text{C}-\text{C})$  are remarkably similar, whereas corrections to  $r(\text{C}-\text{F})$  computed from the MD trajectories are always smaller than those from the SHRINK procedure. The reason for this is unclear. On the one hand, it is well known that classical MD underestimates vibrational amplitudes and corrections for light atom pairs (see ref.<sup>[29,30]</sup>), but corrections for C–C pairs (which have reduced masses even smaller than

C–F) are in very good agreement with SHRINK. On the other hand, in our experience, SHRINK calculations with a cubic force field can sometimes produce unreasonably large corrections for bonded distances in molecules with low-frequency vibrational modes.

Nevertheless, anharmonic vibrational corrections (either from MD or from SHRINK) allow equilibrium bond lengths to be determined from GED experiments that can be directly compared with theoretically calculated values. The calculations of third derivatives for larger molecules requires a prohibitively large amount of computational resources and it also scales very poorly with the system size, so, until recently, the analysis of the GED data for such molecules was only possible by using  $k_{h1}$  vibrational corrections (see the discussion in ref.<sup>[32]</sup> for an example). It is also not better than harmonic approaches for the description of modes having even potentials (because cubic force field constants for such modes are zero by symmetry). At the same time, molecular dynamics calculations are possible even for large (more than 100 atoms) molecules and vibrational corrections by this approach are computed directly, without any assumptions about the shape of the governing potential. Therefore the MD approach<sup>[29]</sup> is a valuable method for determining equilibrium structures directly from GED experiments and we also applied it to analyse the GED data for  $(\text{C}_2\text{F}_5)_2\text{POH}$ .

### $(\text{C}_2\text{F}_5)_2\text{POH}$

The  $(\text{C}_2\text{F}_5)_2\text{POH}$  molecule has an additional conformational degree of freedom due to the rotation of the O–H bond around the P–O axis. Therefore each enantiomer can theoretically have 12 conformers: six with hydrogen oriented in the same direction as the two P–C bonds (conform-

ers A) and six with hydrogen oriented in the opposite direction (conformers B). Figure 6 shows the positions of conformers A on the PES and Table 4 contains information on both conformers A and B (data determined at the B3LYP/cc-pVTZ level are available in the Supporting Information). According to the gas-phase study,<sup>[15]</sup> (CF<sub>3</sub>)<sub>2</sub>POH has two conformers with different orientations of the O–H bond in a relative abundance of 82 and 18% at room temperature [IR and computational data for (CF<sub>3</sub>)<sub>2</sub>POH<sup>[15]</sup>]. However, because the scattering ability of hydrogen atoms is very low compared with that of heavier nuclei (C, O, F and P), these rotamers cannot be reliably distinguished by GED. We made an attempt to include conformers with different orientations of the O–H unit in (C<sub>2</sub>F<sub>5</sub>)<sub>2</sub>POH in the analysis, but the disagreement factor *R<sub>f</sub>* remained unchanged.

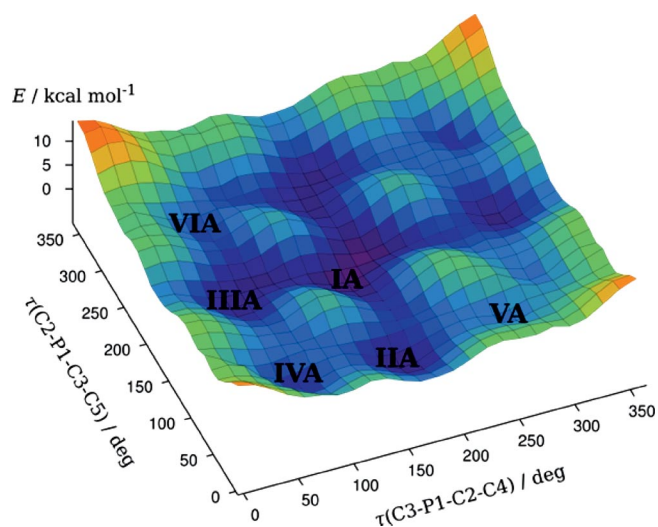


Figure 6. Potential energy surface of (C<sub>2</sub>F<sub>5</sub>)<sub>2</sub>POH for the rotation around two P–C bonds [ $\tau(\text{C}2\text{--P}1\text{--C}3\text{--C}5)$  and  $\tau(\text{C}3\text{--P}1\text{--C}2\text{--C}4)$  dihedral angles] calculated at the B3LYP/6-31++G(d,p) level of theory.

Table 4. Conformers of (C<sub>2</sub>F<sub>5</sub>)<sub>2</sub>POH, their torsion angles, relative energies and abundances at 295.15 K calculated at the O3LYP/aug-cc-pVTZ level of theory.<sup>[a]</sup>

Conf.	$\tau(\text{C}2\text{--P}1\text{--C}3\text{--C}5)$ [°]	$\tau(\text{C}3\text{--P}1\text{--C}2\text{--C}4)$ [°]	$\Delta E$ [kcal mol <sup>-1</sup> ]	$\Delta G^\circ$ [kcal mol <sup>-1</sup> ]	<i>x</i> [mol-%]
IA	164.6	168.4	0.00	0.00	60.7
IB	167.8	166.1	1.22	0.85	14.4
IIA	62.2	170.4	0.97	1.04	10.5
IIIB	69.5	167.0	2.10	1.63	3.9
IIIA	167.0	50.0	0.61	1.31	6.6
IIIB	168.7	47.7	1.77	1.94	2.3
IVA	70.8	49.5	2.08	2.68	0.7
IVB	75.7	45.4	2.96	3.22	0.3
VA	70.2	-107.6	2.54	2.91	0.4
VB	75.0	-109.8	3.27	3.45	0.2
VIA	-99.2	58.7	3.88	4.83	0.0
VIB	-94.5	54.8	4.30	4.82	0.0

[a] Conformers A have H atoms oriented in the same direction as the two P–C bonds, conformers B have H atoms oriented in the opposite direction.

Therefore, to keep the model from being overcomplicated, we limited the analysis to the two lowest-energy conformers with the same orientation of O–H, IA and IIA (see Figure 7), as in the case of (C<sub>2</sub>F<sub>5</sub>)<sub>2</sub>PH.

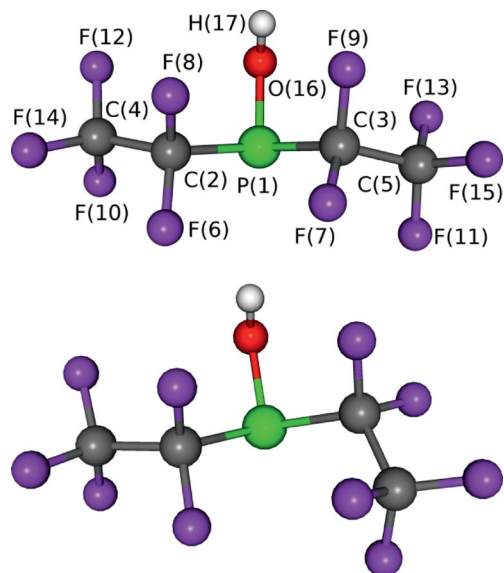


Figure 7. Calculated molecular structures of conformers IA and IIA of (C<sub>2</sub>F<sub>5</sub>)<sub>2</sub>POH.

The refinement with *k<sub>MD</sub>* corrections yielded the disagreement factor *R<sub>f</sub>* = 5.2%. The refined amount of conformer IIA was 15(6) mol-% (the 3 $\sigma_{\text{LS}}$  uncertainty is shown in parentheses), which is in agreement with the amount of IIA conformer (and also with the combined amount of IIA and IIIB conformers) predicted by computation. The major refined structural parameters of (C<sub>2</sub>F<sub>5</sub>)<sub>2</sub>POH obtained from the GED experiment as well as the parameters calculated at the O3LYP and MP2 levels of theory are listed in Table 5, radial distribution *f(r)* curves are presented in Figure 8 and molecular intensity *sM(s)* curves are available in the Supporting Information.

The calculated P–C and C–C bond lengths are overestimated in the O3LYP/aug-cc-pVTZ computations with differences larger than the experimental errors, but MP2/aug-cc-pVTZ yielded values close to the experimental ones. The calculated values of the P–O bond length are too large at all levels of theory. The O3LYP/aug-cc-pVTZ approximation gives C–F distances that are very slightly elongated (by 0.003 Å). It seems that this compound is also a difficult case for quantum chemistry like (C<sub>2</sub>F<sub>5</sub>)<sub>2</sub>PH.

Again, we can compare the bond lengths of the major conformer to those of (C<sub>2</sub>F<sub>5</sub>)<sub>2</sub>PCL studied previously by GED.<sup>[4]</sup> The *r<sub>g</sub>*(P–C) distances in (C<sub>2</sub>F<sub>5</sub>)<sub>2</sub>POH [1.909(3) and 1.911(3) Å] are virtually the same (within experimental uncertainties) as in (C<sub>2</sub>F<sub>5</sub>)<sub>2</sub>PCL, whereas the *r<sub>g</sub>*(C–C) distances [1.549(3) and 1.551(3) Å] are longer on average (by 0.022 Å). The average *r<sub>g</sub>*(C–F) = 1.347(1) Å for CF<sub>2</sub> and *r<sub>g</sub>*(C–F) = 1.328(1) Å for CF<sub>3</sub> are slightly shorter (by 0.004 Å) than those in (C<sub>2</sub>F<sub>5</sub>)<sub>2</sub>PCL.<sup>[4]</sup>

Table 5. Major structural parameters of the  $(C_2F_5)_2POH$  molecule.<sup>[a]</sup>

	Conformer IA			Conformer IIA		
	GED $r_e$ ( $k_{MD}$ )	O3LYP/aug-cc-pVTZ $r_e$	MP2/aug-cc-pVTZ $r_e$	GED $r_e$ ( $k_{MD}$ )	O3LYP/aug-cc-pVTZ $r_e$	MP2/aug-cc-pVTZ $r_e$
$r(P1-C2)$	1.888(3) <sup>g1</sup>	1.917	1.892	1.886(3)	1.915	1.891
$r(P1-C3)$	1.900(3) <sup>g1</sup>	1.928	1.904	1.896(3)	1.925	1.901
$r(P1-O16)$	1.582(3) <sup>g2</sup>	1.623	1.627	1.583(3)	1.624	1.628
$r(C2-C4)$	1.530(3) <sup>g2</sup>	1.548	1.531	1.529(3)	1.547	1.531
$r(C3-C5)$	1.526(3) <sup>g2</sup>	1.544	1.527	1.526(3)	1.544	1.530
$r(C2-F6)$	1.342(1) <sup>g3</sup>	1.345	1.351	1.344(1)	1.347	1.353
$r(C2-F8)$	1.347(1) <sup>g3</sup>	1.350	1.355	1.346(1)	1.349	1.355
$r(C3-F7)$	1.337(1) <sup>g3</sup>	1.340	1.346	1.346(1)	1.349	1.354
$r(C3-F9)$	1.349(1) <sup>g3</sup>	1.352	1.356	1.348(1)	1.351	1.356
$r(C4-F10)$	1.326(1) <sup>g3</sup>	1.329	1.332	1.326(1)	1.329	1.331
$r(C4-F12)$	1.325(1) <sup>g3</sup>	1.328	1.329	1.325(1)	1.328	1.329
$r(C4-F14)$	1.323(1) <sup>g3</sup>	1.326	1.326	1.323(1)	1.326	1.326
$r(C5-F11)$	1.324(1) <sup>g3</sup>	1.328	1.330	1.321(1)	1.324	1.325
$r(C5-F13)$	1.327(1) <sup>g3</sup>	1.330	1.333	1.328(1)	1.331	1.334
$r(C5-F15)$	1.322(1) <sup>g3</sup>	1.325	1.325	1.323(1)	1.327	1.327
$\alpha(C2-P1-C3)$	92.7(5)	95.0	93.4	97.0(5)	99.3	97.4
$\alpha(C4-C2-P1)$	112.9(3)	112.7	112.7	112.9(3)	112.7	112.8
$\alpha(C5-C3-P1)$	111.5(3)	111.3	111.1	119.6(3)	119.4	118.7
$\tau(C4-C2-C1-C3)$	177(3)	168.3	164.9	179(3)	170.4	168.4
$\tau(C5-C3-P1-C2)$	173(3)	164.5	164.5	71(3)	62.2	59.8

[a] The uncertainties quoted in parentheses are  $3\sigma_{LS}$ . Bond lengths of the same kind were varied in groups g1–g3 with fixed differences (see the Exp. Sect. for details) and therefore the  $3\sigma_{LS}$  uncertainties represent least-squares analysis errors of these groups, not individual bond lengths. Distances are given in Å and angles in degrees.

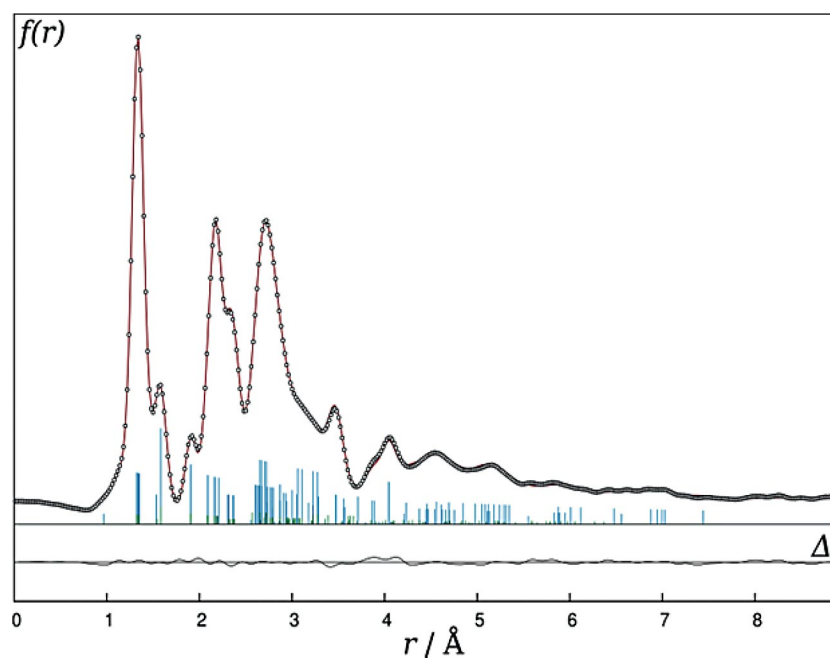


Figure 8. Experimental (dots) and theoretical (line) radial distribution  $f(r)$  curves and difference curve (below) for  $(C_2F_5)_2POH$ . Vertical bars indicate the interatomic distances.

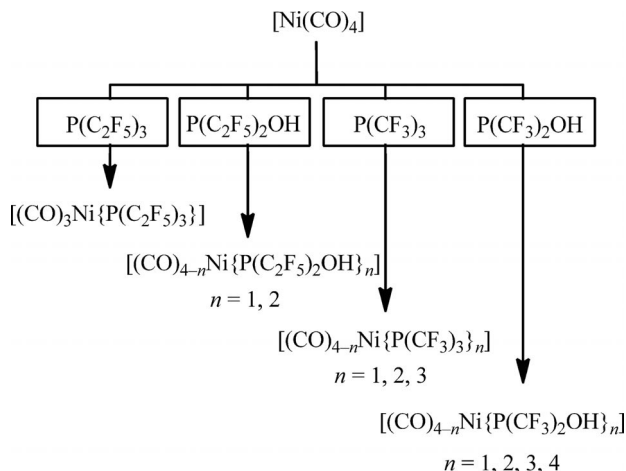
### Evaluation of the Steric Demand by Complex Formation

To demonstrate the different coordination properties of  $(C_2F_5)_3P$ ,  $(C_2F_5)_2POH$ ,  $(CF_3)_3P$  and  $(CF_3)_2POH$ , in particular, with respect to their spatial requirements, we investigated their kinetically controlled reactions with  $[Ni(CO)_4]$  in  $CH_2Cl_2$  solution. The reaction of an excess of  $(C_2F_5)_3P$  with  $[Ni(CO)_4]$  led to the formation and isolation of the first example of a transition-metal complex bearing the

$(C_2F_5)_3P$  ligand, namely  $[(CO)_3Ni\{P(C_2F_5)_3\}]$ . The huge steric demand of  $(C_2F_5)_3P$  prevented substitution of a second CO ligand by this phosphane. This led to the exclusive formation of  $[(CO)_3Ni\{P(C_2F_5)_3\}]$ , even when  $[Ni(CO)_4]$  was treated with a large excess of  $(C_2F_5)_3P$  over a long period of time.

In contrast, the less sterically demanding phosphinous acid  $(C_2F_5)_2POH$  as well as  $(CF_3)_3P$  allowed the substitution of two CO ligands in  $[Ni(CO)_4]$ . This led to the forma-

tion of the corresponding dicarbonyl bis-phosphane complexes (cf. Scheme 2). The even smaller steric demand of  $(\text{CF}_3)_2\text{POH}$  was demonstrated by the substitution of all four CO ligands by phosphane units to afford  $[\text{Ni}\{\text{P}(\text{CF}_3)_2\text{OH}\}_4]$  under the same reaction conditions.



Scheme 2. Observed complex formation in the reaction of  $[\text{Ni}(\text{CO})_4]$  with an excess of different perfluoroalkylphosphane derivatives.

The complex  $[\text{Ni}(\text{CO})_3\{\text{P}(\text{CF}_3)_2\text{OH}\}]$  is a colourless liquid. A single crystal with one water molecule per formula unit was obtained by in situ crystallization. This was

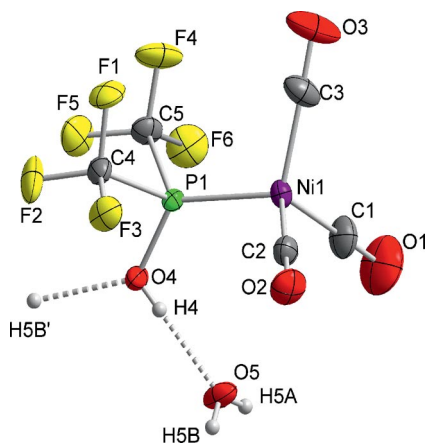


Figure 9. Molecular structure of  $[\text{Ni}(\text{CO})_3\{\text{P}(\text{CF}_3)_2\text{OH}\}]\cdot\text{H}_2\text{O}$  in the solid state. Non-hydrogen atoms are shown as displacement ellipsoids at the 50% probability level. Selected bond lengths [Å] and angles [°]: P1–Ni1 2.123(1), P1–C4 1.883(2), P1–C5 1.881(2), Ni1–C1 1.823(2), P1–O4 1.591(2), O4–O5 2.514(2), C5–F4 1.330(3); C4–P1–C5 97.1(1), Ni1–P1–O4 123.9(1).

achieved by first establishing a solid/liquid equilibrium close to the melting point at 281.2 K, then melting all the solid except for a tiny crystal seed (by using a thin copper wire as external heat source) followed by very slowly lowering the temperature until the whole capillary was filled with a single crystalline specimen. Figure 9 shows a part of the crystal structure with hydrogen-bridged chains. In agreement with the VSEPR model, the C–P–C and O–P–C angles are reduced compared with in the free phosphinous acid<sup>[13c,15]</sup> by around 2° due to the coordination to the  $\text{Ni}(\text{CO})_3$  fragment. On the other hand, such a moderate change in angles can be attributed to packing effects in the crystal. The P–C and P–O distances are reduced as well by about 0.02 Å upon coordination.

## Conclusions

Bis(pentafluoroethyl)phosphane derivatives are well-suited starting materials for the synthesis of a variety of electron-deficient and  $\pi$ -acidic ligands. Starting from non-toxic, commercially available  $\text{C}_2\text{F}_5\text{H}$  with zero ozone depletion potential, the minor air- and moisture-sensitive aminophosphane  $(\text{C}_2\text{F}_5)_2\text{PNET}_2$  is accessible on a multi-gram scale. It serves as a convenient starting material for the selective synthesis of bis(pentafluoroethyl)phosphane derivatives  $(\text{C}_2\text{F}_5)_2\text{PX}$  (X = H, Cl, OH) and the efficient synthesis of the hitherto unknown compounds  $(\text{C}_2\text{F}_5)_2\text{PF}$  and  $(\text{C}_2\text{F}_5)_2\text{PBr}$ . Bis(pentafluoroethyl)phosphane is a synthon for nucleophilic bis(pentafluoroethyl)phosphanides, as shown by the preparation of the complex  $[\text{Hg}\{\text{P}(\text{C}_2\text{F}_5)_2\}_2(\text{dpe})]$ , whereas the halide derivatives  $(\text{C}_2\text{F}_5)_2\text{PX}$  (X = F, Cl, Br) can be synthetically used as electrophilic bis(pentafluoroethyl)phosphonium synthons.

The gas-phase structures of  $(\text{C}_2\text{F}_5)_2\text{PH}$  and  $(\text{C}_2\text{F}_5)_2\text{POH}$  were determined by electron diffraction. A recently developed approach to the treatment of vibrational corrections by molecular dynamics calculations was used in these structural analyses. For comparison, the average structural parameters for these compounds as well as for  $(\text{C}_2\text{F}_5)_2\text{PCl}$  and  $(\text{C}_2\text{F}_5)_3\text{P}$  are listed in Table 6. For the first three entries, the functionalized  $(\text{C}_2\text{F}_5)_2\text{PX}$  compounds, no significant variation in the P–C and C–F bond lengths can be observed, however, some slight variations can be seen in the C–C distances.

A comparison between  $(\text{C}_2\text{F}_5)_2\text{POH}$  in the gaseous and solid phases also shows that in this case typical parameters are rather invariant, for example, the P–C bonds [solid 1.902(2) Å, average] or C–P–C angles [solid 95.3(1)°].<sup>[13c]</sup> In

Table 6. Average structural parameters for  $(\text{C}_2\text{F}_5)_2\text{PX}$  (X = H, OH, Cl,  $\text{C}_2\text{F}_5$ ).

	$(\text{C}_2\text{F}_5)_2\text{PH}$ , $r_e$ ( $k_{\text{MD}}$ )	$(\text{C}_2\text{F}_5)_2\text{POH}$ , $r_e$ ( $k_{\text{MD}}$ )	$(\text{C}_2\text{F}_5)_2\text{PCl}$ , <sup>[a]</sup> $r_{\text{h1}}$	$\text{P}(\text{C}_2\text{F}_5)_3$ , <sup>[b]</sup> $r_{\text{h1}}$
P–C [Å]	1.884(3)	1.891(3)	1.902(3)	1.904(3)
C–C [Å]	1.518(3)	1.528(3)	1.544(3)	1.533(3)
C–F [Å]	1.344(1)	1.333(1)	1.333(1)	1.339(1)
C–P–C [°]	98.4(8)	97.0(5)	98.2(4)	99.9(3)
P–C–C [°]	112.2(2)	112.2(3)	112.8(3)	113.2(3)

[a] See ref.<sup>[4]</sup> [b] See ref.<sup>[3]</sup>

contrast, the P–O distances are significantly different, that is, 1.583(3) Å in the gas and 1.629(1) Å in the solid state. However, in the latter case, the P–OH function acts as a hydrogen bridge in the aggregation of (C<sub>2</sub>F<sub>5</sub>)<sub>2</sub>POH into tetramers.

Together with earlier studies on (C<sub>2</sub>F<sub>5</sub>)<sub>3</sub>P, the structure determination in this contribution provides information on the steric requirements of (C<sub>2</sub>F<sub>5</sub>)<sub>3</sub>P and (C<sub>2</sub>F<sub>5</sub>)<sub>2</sub>POH as ligands in complex chemistry. These data are augmented by complex formation studies of these ligands and their trifluoromethyl analogues (CF<sub>3</sub>)<sub>3</sub>P and (CF<sub>3</sub>)<sub>2</sub>POH in substitution reactions with [Ni(CO)<sub>4</sub>], which revealed the order of effective size: (C<sub>2</sub>F<sub>5</sub>)<sub>3</sub>P > (C<sub>2</sub>F<sub>5</sub>)<sub>2</sub>POH ≈ (CF<sub>3</sub>)<sub>3</sub>P > (CF<sub>3</sub>)<sub>2</sub>POH.

## Experimental Section

**General:** All chemicals were obtained from commercial sources and used without further purification. Standard high-vacuum techniques were employed throughout all preparative procedures. Non-volatile compounds were handled under dry N<sub>2</sub> by using Schlenk techniques. The NMR spectra were recorded with a Bruker Model Avance III 300 spectrometer (<sup>31</sup>P: 111.92 MHz; <sup>19</sup>F: 282.40 MHz; <sup>13</sup>C: 75.47 MHz, <sup>1</sup>H: 300.13 MHz) with positive shifts (in ppm) downfield from the external standards [85% orthophosphoric acid (<sup>31</sup>P), CCl<sub>3</sub>F (<sup>19</sup>F) and TMS (<sup>1</sup>H)]. IR spectra were recorded with an ALPHA-FT-IR spectrometer (Bruker) by using a gas cell with KBr windows.

**Synthesis of (C<sub>2</sub>F<sub>5</sub>)<sub>2</sub>PNEt<sub>2</sub>:** *Caution!* LiC<sub>2</sub>F<sub>5</sub> is highly reactive and tends to decompose violently at temperatures above –50 °C.

A 1.6 M *n*-butyllithium solution in *n*-hexane (141 mL, 226 mmol) dissolved in diethyl ether (400 mL) was degassed at –78 °C and the solution was stirred for 30 min in an atmosphere of pentafluoroethane (230 mmol). After the addition of dichloro(diethylamino)phosphane (18.1 g, 104 mmol) at –78 °C, the mixture was warmed to room temperature and stirred overnight. The precipitate was removed by filtration. After evaporation of the solvent, 24.6 g (72.1 mmol, 69%) of (C<sub>2</sub>F<sub>5</sub>)<sub>2</sub>PNEt<sub>2</sub> was obtained by vacuum distillation at 33–35 °C as a colourless liquid. <sup>1</sup>H NMR (C<sub>6</sub>D<sub>6</sub>, 20 °C): δ = 1.3 [t, <sup>2</sup>J(H,H) = 6.9 Hz, CH<sub>3</sub>], 3.3 [q, <sup>2</sup>J(H,H) = 6.9 Hz, CH<sub>2</sub>] ppm. <sup>13</sup>C{<sup>1</sup>H} NMR (C<sub>6</sub>D<sub>6</sub>, 20 °C): δ = 46.9 [d, <sup>2</sup>J(C,P) = 43 Hz, CH<sub>2</sub>], 12.6 (m, CH<sub>3</sub>) ppm. <sup>13</sup>C{<sup>19</sup>F} NMR (C<sub>6</sub>D<sub>6</sub>, 20 °C): δ = 119.4 [d, <sup>2</sup>J(C,P) = 25 Hz, CF<sub>3</sub>], 118.5 [d, <sup>1</sup>J(C,P) = 58 Hz, CF<sub>2</sub>] ppm. <sup>19</sup>F NMR (C<sub>6</sub>D<sub>6</sub>, 20 °C): δ = –82.1 [d, <sup>3</sup>J(P,F) = 18 Hz, CF<sub>3</sub>], –116.1/–117 (m, CF<sub>2</sub>) ppm. <sup>31</sup>P{<sup>1</sup>H} NMR (C<sub>6</sub>D<sub>6</sub>, 20 °C): δ = 46.8 (m) ppm. IR (gas phase): ν̄ = 405 (vw), 445 (vw), 470 (vw), 618 (vw), 746 (w), 797 (vw), 947 (m), 1035 (w), 1059 (vw), 1126 (m), 1145 (m), 1171 (w), 1224 (s), 1301 (m), 1389 (w), 1472 (vw), 2889 (vw), 2951 (vw), 2980 (vw) cm<sup>–1</sup>.

**Synthesis of (C<sub>2</sub>F<sub>5</sub>)<sub>2</sub>PCl:** (C<sub>2</sub>F<sub>5</sub>)<sub>2</sub>PNEt<sub>2</sub> (9.1 g, 27 mmol) was cooled to –30 °C and degassed for 5 min. Under vigorous stirring, gaseous HCl was slowly added. All volatile compounds were removed by condensation and the condensate was repeatedly treated with gaseous HCl until no further precipitation of ammonium salts was observed. Excess HCl was removed in vacuo at –78 °C yielding 6.9 g (23 mmol, 85%) of a colourless liquid. <sup>19</sup>F NMR (CDCl<sub>3</sub>, 20 °C): δ = –80.2 [d, <sup>3</sup>J(P,F) = 16 Hz, CF<sub>3</sub>], –115.9 (m, CF<sub>2</sub>) ppm. <sup>31</sup>P NMR (CDCl<sub>3</sub>, 20 °C): δ = 62.2 (m) ppm. IR (gas phase): ν̄ = 532 (w), 555 (w), 749 (w), 951 (m), 1117 (w), 1141 (w), 1169 (m), 1230 (s), 1304 (m) cm<sup>–1</sup>.

**Synthesis of (C<sub>2</sub>F<sub>5</sub>)<sub>2</sub>PBr:** (C<sub>2</sub>F<sub>5</sub>)<sub>2</sub>PNEt<sub>2</sub> (2.5 g, 7.2 mmol) was cooled to –30 °C and degassed for 5 min. Under vigorous stirring, gaseous HBr was slowly added. All volatile compounds were removed by condensation and the condensate was repeatedly treated with gaseous HBr until no further precipitation of ammonium salts was observed. Excess HBr was removed in vacuo at –78 °C yielding 1.8 g (5.1 mmol, 70%) of a colourless liquid. <sup>13</sup>C{<sup>19</sup>F} NMR (Et<sub>2</sub>O, 20 °C): δ = 119.1 [d, <sup>2</sup>J(C,P) = 22 Hz, CF<sub>3</sub>], 116.0 [d, <sup>1</sup>J(C,P) = 69 Hz, CF<sub>2</sub>] ppm. <sup>19</sup>F NMR (Et<sub>2</sub>O, 20 °C): δ = –80.6 [m, d, <sup>3</sup>J(P,F) = 17 Hz], –112.0/–114.1 (m, CF<sub>2</sub>) ppm. <sup>31</sup>P NMR (Et<sub>2</sub>O, 20 °C): δ = 44.0 (m) ppm. IR (gas phase): ν̄ = 612 (w), 628 (w), 749 (m), 949 (m), 1111 (w), 1137 (w), 1167 (m), 1230 (s), 1302 (m) cm<sup>–1</sup>.

**Synthesis of (C<sub>2</sub>F<sub>5</sub>)<sub>2</sub>PF:** (C<sub>2</sub>F<sub>5</sub>)<sub>2</sub>PBr (1.4 g, 4.0 mmol) was condensed onto an excess of antimony trifluoride, dried in vacuo for 1 h. The reaction mixture was stirred at room temperature for 48 h and 1.0 g (3.6 mmol, 90%) of the volatile product was removed by condensation. <sup>13</sup>C{<sup>19</sup>F} NMR (Et<sub>2</sub>O, 20 °C): δ = 119.1 [d, <sup>2</sup>J(C,P) = 20 Hz, CF<sub>3</sub>], 116.6 [dd, <sup>1</sup>J(C,P) = 57, <sup>2</sup>J(C,F) = 8 Hz, CF<sub>2</sub>] ppm. <sup>19</sup>F NMR (Et<sub>2</sub>O, 20 °C): δ = –82.4 [dd, <sup>3</sup>J(P,F) = 13, <sup>4</sup>J(F,F) = 6 Hz, CF<sub>3</sub>], –123.7/–125.0 (m, CF<sub>2</sub>), –216.7 [m, d, <sup>1</sup>J(P,F) = 1015 Hz, F] ppm. <sup>31</sup>P{<sup>1</sup>H} NMR (Et<sub>2</sub>O, 20 °C): δ = 137.6 [m, d, <sup>1</sup>J(P,F) = 1015 Hz] ppm. IR (gas phase): ν̄ = 610 (vw), 628 (w), 751 (vw), 864 (w), 959 (w), 1029 (m), 1171 (m), 1231 (s), 1309 (m) cm<sup>–1</sup>.

**Synthesis of (C<sub>2</sub>F<sub>5</sub>)<sub>2</sub>PH:** (C<sub>2</sub>F<sub>5</sub>)<sub>2</sub>PCl (5.8 g, 19 mmol) was condensed onto degassed Bu<sub>3</sub>SnH (6.0 g, 21 mmol). The two-phase system was stirred at room temperature for 1 h and the product was removed under static vacuum yielding 5.2 g (19 mmol, 100%) of a colourless liquid. <sup>1</sup>H NMR (Et<sub>2</sub>O, 20 °C): δ = 5.2 [m, d, <sup>1</sup>J(P,H) = 231 Hz] ppm. <sup>13</sup>C NMR (Et<sub>2</sub>O, 20 °C): δ = 119.1 [m, t, <sup>1</sup>J(C,F) = 289 Hz, CF<sub>2</sub>], 118.9 [m, q, <sup>1</sup>J(C,F) = 285 Hz, CF<sub>3</sub>] ppm. <sup>13</sup>C{<sup>19</sup>F} NMR (Et<sub>2</sub>O, 20 °C): δ = 119.1 [m, d, <sup>1</sup>J(C,P) = 39 Hz, CF<sub>2</sub>], 118.9 [m, d, <sup>2</sup>J(C,P) = 19 Hz, CF<sub>3</sub>] ppm. <sup>19</sup>F NMR (Et<sub>2</sub>O, 20 °C): δ = –84.8 [m, d, <sup>3</sup>J(P,F) = 13 Hz, CF<sub>3</sub>], –103.0/–109.0 (m, CF<sub>2</sub>) ppm. <sup>31</sup>P NMR (Et<sub>2</sub>O, 20 °C): δ = –50.8 [m, d, <sup>1</sup>J(P,H) = 231 Hz] ppm. IR (gas phase): ν̄ = 404 (vw), 608 (w), 748 (m), 855 (vw), 961 (m), 990 (w), 1004 (w), 1155 (m), 1230 (s), 1312 (m), 2349 (vw) cm<sup>–1</sup>.

**Synthesis of (C<sub>2</sub>F<sub>5</sub>)<sub>2</sub>POH:** (C<sub>2</sub>F<sub>5</sub>)<sub>2</sub>PNEt<sub>2</sub> (4.1 g, 11.9 mmol) was added to a suspension of *p*-toluenesulfonic acid monohydrate (15.5 g, 81.5 mmol) in 1,6-dibromohexane (75 mL), dried and degassed in vacuo for 1 h. The reaction mixture was stirred at room temperature for 48 h resulting in a rose-coloured suspension. The volatile compounds were removed under dynamic vacuum conditions using three traps at –30, –78 and –196 °C to separate minor amounts of the solvent, (C<sub>2</sub>F<sub>5</sub>)<sub>2</sub>POH and C<sub>2</sub>F<sub>5</sub>H. The –78 °C trap contained 3.2 g (11.1 mmol, 93%) of a colourless liquid identified as (C<sub>2</sub>F<sub>5</sub>)<sub>2</sub>POH. <sup>1</sup>H NMR (CDCl<sub>3</sub>, 20 °C): δ = 3.3 (s) ppm. <sup>13</sup>C{<sup>19</sup>F} NMR (CDCl<sub>3</sub>, 20 °C): δ = 119.2 [d, <sup>2</sup>J(C,P) = 20 Hz, CF<sub>3</sub>], 117.3 (m, CF<sub>2</sub>) ppm. <sup>19</sup>F NMR (CDCl<sub>3</sub>, 20 °C): δ = –82.1 [m, d, <sup>3</sup>J(P,F) = 18 Hz, CF<sub>3</sub>], –123.4/–125.4 (m, CF<sub>2</sub>) ppm. <sup>31</sup>P NMR (CDCl<sub>3</sub>, 20 °C): δ = 93.0 (m) ppm.

**General Procedure for the Investigation of the Coordination Properties of P(C<sub>2</sub>F<sub>5</sub>)<sub>3</sub>, P(CF<sub>3</sub>)<sub>3</sub>, (C<sub>2</sub>F<sub>5</sub>)<sub>2</sub>POH and (CF<sub>3</sub>)<sub>2</sub>POH by Kinetically Controlled Reactions with [Ni(CO)<sub>4</sub>]:** Four equivalents of the phosphane derivative were condensed onto a solution of nickel tetracarbonyl in CH<sub>2</sub>Cl<sub>2</sub>. After stirring for 24 h, the progress of the reaction was monitored by IR and NMR spectroscopy (some of the NMR spectra are of higher order, in these cases best estimates of the coupling constants are provided.).

**[Ni(CO)<sub>3</sub>](P(C<sub>2</sub>F<sub>5</sub>)<sub>3</sub>):** <sup>31</sup>P NMR (CH<sub>2</sub>Cl<sub>2</sub>, [D<sub>6</sub>]acetone ext. lock, 20 °C): δ = 56.7 [sept, decet, <sup>2</sup>J(P,F) = 60, <sup>3</sup>J(P,F) = 6 Hz] ppm. <sup>19</sup>F

NMR (CH<sub>2</sub>Cl<sub>2</sub>, [D<sub>6</sub>]acetone ext. lock, 20 °C):  $\delta$  = -78.5 [d, <sup>3</sup>J(P,F)] = 6 Hz, CF<sub>3</sub>], -106.9 [d, <sup>2</sup>J(P,F)] = 60 Hz, CF<sub>2</sub>] ppm. IR (CH<sub>2</sub>Cl<sub>2</sub>):  $\tilde{\nu}$  = 2110 [m,  $\nu_s$ (CO)], 2051 [vs,  $\nu_{as}$ (CO)] cm<sup>-1</sup>. IR (gas phase):  $\tilde{\nu}$  = 2114 [m,  $\nu_s$ (CO)], 2060 [s,  $\nu_{as}$ (<sup>12</sup>CO)], 2023 [w,  $\nu_{as}$ (<sup>13</sup>CO)], 1303 [s,  $\nu$ (CC)], 1237 [vs,  $\nu$ (CF), CF<sub>3</sub>], 1172 [s,  $\nu$ (CF), CF<sub>2</sub>], 1107 [w,  $\nu$ (CF), CF<sub>2</sub>], 950 [s,  $\nu$ (PC)], 751 [w,  $\delta$ (CF<sub>3</sub>)], 630 (w) cm<sup>-1</sup>. MS (EI-TOF, pos., 30 eV): *m/z* (%) = 529.9 (33) [M]<sup>+</sup>, 501.9 (88) [M - CO]<sup>+</sup>, 473.9 (74) [M - 2CO]<sup>+</sup>, 454.9 (31) [M - 3CO]<sup>+</sup>; 387.9 (16) [P(C<sub>2</sub>F<sub>5</sub>)<sub>3</sub>]<sup>+</sup>, 141.9 (100) [Ni(CO)<sub>3</sub>]<sup>+</sup>, 118.9 (32) [C<sub>2</sub>F<sub>5</sub>]<sup>+</sup>, 113.9 (33) [Ni(CO)<sub>2</sub>]<sup>+</sup>, 100 (31) [C<sub>2</sub>F<sub>4</sub>]<sup>+</sup>, 58 (18) [Ni]<sup>+</sup>.

[Ni(CO)<sub>3</sub>{P(CF<sub>3</sub>)<sub>3</sub>}]<sup>+</sup>: <sup>31</sup>P NMR (CDCl<sub>3</sub>, 20 °C):  $\delta$  = 50.3 [decet, <sup>2</sup>J(P,F)] = 87 Hz] ppm. <sup>19</sup>F NMR (CDCl<sub>3</sub>, 20 °C):  $\delta$  = -58.4 [d, <sup>2</sup>J(P,F)] = 87 Hz] ppm. IR (CH<sub>2</sub>Cl<sub>2</sub>):  $\tilde{\nu}$  = 2110 [m,  $\nu_s$ (CO)], 2037 [vs,  $\nu_{as}$ (CO)] cm<sup>-1</sup>.

[Ni(CO)<sub>2</sub>{P(CF<sub>3</sub>)<sub>3</sub>}<sub>2</sub>]<sup>+</sup>: <sup>31</sup>P NMR (CDCl<sub>3</sub>, 20 °C):  $\delta$  = 52.0 [m, <sup>2</sup>J(P,F)] = 93 Hz] ppm. <sup>19</sup>F NMR (CDCl<sub>3</sub>, 20 °C):  $\delta$  = -56.8 [m, <sup>2</sup>J(P,F)] = 93 Hz] ppm. IR (CH<sub>2</sub>Cl<sub>2</sub>):  $\tilde{\nu}$  = 2096 [ $\nu_{as}$ (CO)] cm<sup>-1</sup>.

[Ni(CO)<sub>3</sub>{P(C<sub>2</sub>F<sub>5</sub>)<sub>2</sub>OH}]<sup>+</sup>: <sup>31</sup>P NMR (CDCl<sub>3</sub>, 20 °C):  $\delta$  = 119.2 [m, <sup>2</sup>J(P,F)] = 73 Hz] ppm. <sup>19</sup>F NMR (CDCl<sub>3</sub>, 20 °C):  $\delta$  = -78.7 (m, CF<sub>3</sub>), -121.3 [m, <sup>2</sup>J(P,F)] = 73 Hz, CF<sub>2</sub>] ppm. IR (CH<sub>2</sub>Cl<sub>2</sub>):  $\tilde{\nu}$  = 2100 [m,  $\nu_s$ (CO)], 2036 [vs,  $\nu_{as}$ (CO)] cm<sup>-1</sup>.

[Ni(CO)<sub>2</sub>{P(C<sub>2</sub>F<sub>5</sub>)<sub>2</sub>OH}]<sub>2</sub><sup>+</sup>: <sup>31</sup>P NMR (CDCl<sub>3</sub>, 20 °C):  $\delta$  = 124.6 [m, <sup>2</sup>J(P,F)] = 73 Hz] ppm. <sup>19</sup>F NMR (CDCl<sub>3</sub>, 20 °C):  $\delta$  = -78.4 (m, CF<sub>3</sub>), -124.6 [m, <sup>2</sup>J(P,F)] = 83 Hz, CF<sub>2</sub>] ppm.

[Ni(CO)<sub>3</sub>{P(CF<sub>3</sub>)<sub>2</sub>OH}]<sup>+</sup>: <sup>31</sup>P NMR (CDCl<sub>3</sub>, 20 °C):  $\delta$  = 112.6 [sept, <sup>2</sup>J(P,F)] = 91 Hz] ppm. <sup>19</sup>F NMR (CDCl<sub>3</sub>, 20 °C):  $\delta$  = -70.3 [d, <sup>2</sup>J(P,F)] = 91 Hz] ppm. IR (CH<sub>2</sub>Cl<sub>2</sub>):  $\tilde{\nu}$  = 2102 [m,  $\nu_s$ (CO)], 2038 [vs,  $\nu_{as}$ (CO)] cm<sup>-1</sup>.

[Ni(CO)<sub>2</sub>{P(CF<sub>3</sub>)<sub>2</sub>OH}]<sub>2</sub><sup>+</sup>: <sup>31</sup>P NMR (CDCl<sub>3</sub>, 20 °C):  $\delta$  = 115.1 [m, <sup>2</sup>J(P,F)] = 93 Hz] ppm. <sup>19</sup>F NMR (CDCl<sub>3</sub>, 20 °C):  $\delta$  = -69.7 [d, <sup>2</sup>J(P,F)] = 93 Hz] ppm. IR (CH<sub>2</sub>Cl<sub>2</sub>):  $\tilde{\nu}$  = 2075 [m,  $\nu_s$ (CO)], 2033 [vs,  $\nu_{as}$ (CO)] cm<sup>-1</sup>.

[Ni(CO){P(CF<sub>3</sub>)<sub>2</sub>OH}]<sub>3</sub><sup>+</sup>: <sup>31</sup>P NMR (CDCl<sub>3</sub>, 20 °C):  $\delta$  = 115.3 [m, <sup>2</sup>J(P,F)] = 91 Hz] ppm. <sup>19</sup>F NMR (CDCl<sub>3</sub>, 20 °C):  $\delta$  = -69.6 [m, <sup>2</sup>J(P,F)] = 91 Hz] ppm. IR (CH<sub>2</sub>Cl<sub>2</sub>):  $\tilde{\nu}$  = 2056 [m,  $\nu$ (CO)] cm<sup>-1</sup>.

[Ni{P(CF<sub>3</sub>)<sub>2</sub>OH}]<sub>4</sub><sup>+</sup>: <sup>31</sup>P NMR (CDCl<sub>3</sub>, 20 °C):  $\delta$  = 115.4 [m, <sup>2</sup>J(P,F)] = 91 Hz] ppm. <sup>19</sup>F NMR (CDCl<sub>3</sub>, 20 °C):  $\delta$  = -69.2 [m, <sup>2</sup>J(P,F)] = 91 Hz] ppm.

**Synthesis of [Hg{P(C<sub>2</sub>F<sub>5</sub>)<sub>2</sub>}(dppe)]:** (C<sub>2</sub>F<sub>5</sub>)<sub>2</sub>PH (8.0 mmol) was condensed onto a solution of [Hg(CN)<sub>2</sub>(dppe)] (1.76 g, 2.7 mmol) in CH<sub>2</sub>Cl<sub>2</sub> and warmed to room temperature. After stirring for 10 min, all the volatile compounds were removed in vacuo yielding 2.98 g (2.6 mmol, 96%) of a light-yellow solid. <sup>1</sup>H NMR (CDCl<sub>3</sub>, 20 °C):  $\delta$  = 2.7 (s, C<sub>2</sub>H<sub>4</sub>), 7.5 (m, C<sub>6</sub>H<sub>5</sub>) ppm. <sup>13</sup>C{<sup>1</sup>H} NMR (CDCl<sub>3</sub>, 20 °C):  $\delta$  = 24.4 (m, C<sub>2</sub>H<sub>4</sub>), 129.4 (s, C-*m*), 130.4 (m, C-*i*), 131.3 (s, C-*p*), 132.5 (m, C-*o*) ppm. <sup>13</sup>C{<sup>19</sup>F} NMR (CDCl<sub>3</sub>, 20 °C):  $\delta$  = 120.0 [d, <sup>2</sup>J(C,P)] = 23 Hz, CF<sub>3</sub>], 124.1 [d, <sup>1</sup>J(C,P)] = 76 Hz, CF<sub>2</sub>] ppm. <sup>19</sup>F NMR (CD<sub>2</sub>Cl<sub>2</sub>, 247 K):  $\delta$  = -83.5 [d, <sup>3</sup>J(P,F)] = 14 Hz, CF<sub>3</sub>], -89.3 [dd, <sup>2</sup>J(F,F)] = 291, <sup>2</sup>J(P,F)] = 65, <sup>3</sup>J(Hg,F)] = 250 Hz, CF<sub>a</sub>F], -98.5 [d, <sup>2</sup>J(F,F)] = 296, <sup>3</sup>J(Hg,F)] = 140 Hz, CFF<sub>b</sub>] ppm. <sup>31</sup>P{<sup>19</sup>F} NMR (CD<sub>2</sub>Cl<sub>2</sub>, 247 K):  $\delta$  = 11.2 [t, <sup>2</sup>J(P,P)] = 57, <sup>1</sup>J(Hg,P)] = 212 Hz, PPH<sub>2</sub>], -9.2 [t, <sup>2</sup>J(P,P)] = 58, <sup>1</sup>J(Hg,P)] = 824 Hz, P(C<sub>2</sub>F<sub>5</sub>)<sub>2</sub>] ppm. <sup>199</sup>Hg{<sup>19</sup>F} NMR (CD<sub>2</sub>Cl<sub>2</sub>, 247 K):  $\delta$  = -296.2 [tt, <sup>1</sup>J(Hg,P<sub>dppe</sub>)] = 209, <sup>1</sup>J(Hg,P<sub>C<sub>2</sub>F<sub>5</sub>)</sub>] = 824] ppm.

**X-ray Crystallography:** Data collections for the X-ray diffraction analyses of [Hg{P(C<sub>2</sub>F<sub>5</sub>)<sub>2</sub>}(dppe)]·C<sub>7</sub>H<sub>8</sub>, [Hg(CN){P(C<sub>2</sub>F<sub>5</sub>)<sub>2</sub>}(dppe)] and [Ni(CO)<sub>3</sub>{P(CF<sub>3</sub>)<sub>2</sub>OH}]·H<sub>2</sub>O were performed with a Bruker-Nonius KappaCCD diffractometer at 100(2) K by using graphite-monochromated Mo-*K*<sub>α</sub> radiation ( $\lambda$  = 0.71073 Å). The structures were solved by direct methods and refined by the full-

matrix least-squares approach.<sup>[33]</sup> All non-hydrogen atoms were refined with anisotropic displacement factors.

**Data for [Hg(CN){P(C<sub>2</sub>F<sub>5</sub>)<sub>2</sub>}(dppe)]:** Colourless crystal, *M*<sub>r</sub> = 986.15, triclinic, space group *P* $\bar{1}$ , *a* = 9.102(1), *b* = 11.776(2), *c* = 18.358(2) Å,  $\alpha$  = 89.34(1),  $\beta$  = 89.07(1),  $\gamma$  = 76.50(1)°, *V* = 1913.0(4) Å<sup>3</sup>, *Z* = 2,  $\rho_{\text{calcd.}}$  = 1.712 g cm<sup>-3</sup>, *F*(000) = 964, 41781 reflections collected up to  $\theta$  = 27.5°, 8734 independent reflections of which 7704 with *I* > 2 $\sigma$ (*I*), 479 parameters. Hydrogen atoms were taken into account at idealized positions by using a riding model. *R* values: *R*<sub>1</sub> = 0.024 for reflections with *I* > 2 $\sigma$ (*I*), *wR*<sub>2</sub> = 0.045 for all data.

**Data for [Hg{P(C<sub>2</sub>F<sub>5</sub>)<sub>2</sub>}(dppe)]·C<sub>7</sub>H<sub>8</sub>:** Colourless crystal, *M*<sub>r</sub> = 1229.14, monoclinic, space group *Pc*, *a* = 9.664(1), *b* = 11.690(1), *c* = 20.679(2) Å,  $\beta$  = 96.49(1)°, *V* = 2321.2(3) Å<sup>3</sup>, *Z* = 2,  $\rho_{\text{calcd.}}$  = 1.759 g cm<sup>-3</sup>, *F*(000) = 1196, 136717 reflections collected up to  $\theta$  = 30°, 13386 independent reflections of which 12286 with *I* > 2 $\sigma$ (*I*), 596 parameters. Hydrogen atoms were taken into account at idealized positions by using a riding model. Hydrogen atoms were refined isotropically. *R* values: *R*<sub>1</sub> = 0.022 for reflections with *I* > 2 $\sigma$ (*I*), *wR*<sub>2</sub> = 0.039 for all data.

**Data for [Ni(CO)<sub>3</sub>{P(CF<sub>3</sub>)<sub>2</sub>OH}]·H<sub>2</sub>O:** Colourless crystal, *M*<sub>r</sub> = 346.75, orthorhombic, space group *Pca*2<sub>1</sub>, *a* = 7.988(1), *b* = 11.855(1), *c* = 12.752(1) Å, *V* = 1207.6(1) Å<sup>3</sup>, *Z* = 4,  $\rho_{\text{calcd.}}$  = 1.907 g cm<sup>-3</sup>, *F*(000) = 680, 21971 reflections collected up to  $\theta$  = 27.0°, 2594 independent reflections of which 2464 with *I* > 2 $\sigma$ (*I*), 177 parameters. *R* values: *R*<sub>1</sub> = 0.018 for reflections with *I* > 2 $\sigma$ (*I*), *wR*<sub>2</sub> = 0.0434 for all data.

CCDC-920714 (for [Hg(CN){P(C<sub>2</sub>F<sub>5</sub>)<sub>2</sub>}(dppe)]·C<sub>7</sub>H<sub>8</sub>), CCDC-920715 (for [Hg{P(C<sub>2</sub>F<sub>5</sub>)<sub>2</sub>}(dppe)]·C<sub>7</sub>H<sub>8</sub>) and CCDC-920716 (for [Ni(CO)<sub>3</sub>{P(CF<sub>3</sub>)<sub>2</sub>OH}]·H<sub>2</sub>O) contain supplementary crystallographic data for this paper. These data can be obtained free of charge from The Cambridge Crystallographic Data Centre via www.ccdc.cam.ac.uk/data\_request/cif.

**Computational Analysis:** Theoretical studies of (C<sub>2</sub>F<sub>5</sub>)<sub>2</sub>PH and (C<sub>2</sub>F<sub>5</sub>)<sub>2</sub>POH were carried out by DFT and Møller–Plesset second-order perturbation theory (MP2) calculations. Preliminary calculations, intended for obtaining starting geometries and Hessian matrices for further higher level computations, as well as for the evaluation of vibrational corrections, were carried out by using the 6-31++G\*\*<sup>[34]</sup> basis sets. In the geometry optimizations and Hessian computations performed by using the B3LYP hybrid functional (referred to as B3LYP/cc-pVTZ), C, H and P atoms were described by the triple- $\zeta$  valence correlation-consistent cc-pVTZ basis sets and F atoms by the aug-cc-pVTZ basis set.<sup>[35]</sup> In calculations performed with the O3LYP hybrid functional and MP2, the aug-cc-pVTZ basis sets<sup>[35]</sup> were used for describing all atoms (these levels of theory are referred to as O3LYP/aug-cc-pVTZ and MP2/aug-cc-pVTZ, respectively). Preliminary calculations and all B3LYP/cc-pVTZ, O3LYP/aug-cc-pVTZ and MP2/aug-cc-pVTZ calculation were performed by using the Firefly 7.1.G QC package,<sup>[36]</sup> which is partially based on the GAMESS (US)<sup>[37]</sup> source code. Third derivatives of the potential energy and two-dimensional potential energy scans along the C–C–P–C torsional angles were calculated by using the Gaussian 03 software<sup>[38]</sup> at the B3LYP/6-31++G\*\* level of theory.

Molecular dynamics (MD) calculations were performed by using the CP2K code.<sup>[39]</sup> The Quickstep method for density functional calculations using a mixed Gaussian and plane waves approach was applied.<sup>[40]</sup> To model an isolated molecule by using this periodic code, a single molecule was simulated in a cubic supercell with a size of 13 Å. The BLYP (Becke–Lee–Yang–Parr) exchange-correlation functional, Goedecker, Teter and Hutter (GTH) pseudopo-

tentials<sup>[41]</sup> and the corresponding DZVP basis sets optimized for the GTH pseudopotentials and the BLYP functional were used. The equilibrium geometries of  $(\text{C}_2\text{F}_5)_2\text{PH}$  (**I** and **II**) and  $(\text{C}_2\text{F}_5)_2\text{POH}$  (conformers **IA** and **IIA**) were optimized starting from the geometries calculated at the 6-31G++(d,p) level, and these structures were subsequently used to determine vibrational corrections by using MD simulations. The simulations were performed in the canonical ensemble(NVT) by using a chain of five Nose–Hoover thermostats with a time constant of 4 fs to regulate the simulation temperature at 300 K, approximately the temperature of the GED experiment. The simulations were performed with a time step of 0.5 fs and lasted for 21 ps [ $(\text{C}_2\text{F}_5)_2\text{PH}$ ] and 20 ps [ $(\text{C}_2\text{F}_5)_2\text{POH}$ ]. The technique for calculating vibrational corrections by using molecular dynamics data is described in refs.<sup>[29,30]</sup>

In this contribution the GED/MD technique<sup>[29]</sup> was further developed to allow computation of vibrational corrections for several conformers, which are present in the same MD trajectory (or several trajectories). Geometries from the trajectories' time steps are classified according to the value of a dihedral or torsional angle such that the conformation and vibrational corrections are computed for each conformer separately by using only geometries that were determined to belong to this particular conformation.

**Electron Diffraction:** Electron scattering intensities for  $(\text{C}_2\text{F}_5)_2\text{PH}$  and  $(\text{C}_2\text{F}_5)_2\text{POH}$  were recorded at room temperature by using a combination of reusable Fuji and Kodak imaging plates and a strongly modified Balzers KD-G2 Gas Eldigraph.<sup>[42]</sup> For both molecules, two sets of electron diffraction patterns were obtained from long ( $L = 500$  mm) and short ( $L = 250$  mm) camera distances at the accelerating voltage of 50 kV [four and three patterns for  $(\text{C}_2\text{F}_5)_2\text{PH}$  and four and six patterns for  $(\text{C}_2\text{F}_5)_2\text{POH}$  from long and short camera distances, respectively]. The data reduction, which yields molecular intensity curves (see the Supporting Information), the electron wavelength determination and the molecular structure refinement were performed by using the UNEX program.<sup>[43]</sup>

Several sets of vibrational corrections were used for the analysis of  $(\text{C}_2\text{F}_5)_2\text{PH}$  data. First,  $k_{\text{h1}}$  corrections from the SHRINK program<sup>[31]</sup> (so-called “second approximation”), calculated by using the B3LYP/cc-pVTZ force field, were used. It is a typical approach for large and flexible molecules successfully used in studies.<sup>[32,44,45]</sup> Secondly, anharmonic corrections computed from the molecular dynamics trajectories<sup>[29,30]</sup> ( $k_{\text{MD}}$ ) were applied. We also calculated third derivatives for the major conformer at the B3LYP/6-31++G\*\* level and computed the anharmonic vibrational corrections by using SHRINK ( $k_3$ ). The Q2SHRINK and SHREx programs<sup>[32]</sup> were used for making input files and extracting data from output files of SHRINK. The  $(\text{C}_2\text{F}_5)_2\text{POH}$  data was analysed by using corrections computed from the molecular dynamics trajectories ( $k_{\text{MD}}$ ).

Nine independent parameters were used in the model of  $(\text{C}_2\text{F}_5)_2\text{PH}$  and were refined by least-squares analysis. The independent distances were  $r(\text{C}2\text{--P}1)$ ,  $r(\text{C}4\text{--C}2)$  and  $r(\text{C}2\text{--F}6)$ , and the differences between  $r(\text{C}2\text{--P}1)$  and  $r(\text{C}3\text{--P}1)$ ,  $r(\text{C}4\text{--C}2)$  and  $r(\text{C}5\text{--C}3)$ ,  $r(\text{C}2\text{--F}6)$  and other  $r(\text{C}\text{--F})$  parameters were fixed at theoretically calculated values. This was justified by the fact that the differences are small and not determinable from the GED data and that the values yielded by calculations at different levels of theory are very similar. Therefore the approach with flexible restraints based on different computations does not have an advantage. Initially, all fixed differences mentioned here were taken from the B3LYP/cc-pVTZ calculations. Then, when we found that the O3LYP/aug-cc-pVTZ values of the bond lengths are closer to the experimental values, we used the differences from these calculations for the final

refinement with  $k_{\text{MD}}$  corrections [and also in the study of  $(\text{C}_2\text{F}_5)_2\text{POH}$ ].

The independent valence angles used were  $\alpha(\text{C}2\text{--P}1\text{--C}3)$ ,  $\alpha(\text{C}4\text{--C}2\text{--P}1)$ ,  $\alpha(\text{F}6\text{--C}2\text{--P}1)$  and  $\alpha(\text{F}10\text{--C}4\text{--C}2)$ ; the differences between  $\alpha(\text{C}4\text{--C}2\text{--P}1)$  and  $\alpha(\text{C}5\text{--C}3\text{--P}1)$  were fixed. The position of the F6 atom was described by the  $\alpha(\text{F}6\text{--C}2\text{--C}4)$  angle, and its difference with  $\alpha(\text{F}6\text{--C}2\text{--P}1)$  was fixed. The F7, F8 and F9 atoms were described in a similar manner with all differences of angles also fixed. The  $\gamma(\text{C}4\text{--C}2\text{--P}1\text{--C}3)$  and  $\gamma(\text{F}10\text{--C}4\text{--C}2\text{--P}1)$  dihedral angles were independent parameters; the differences between  $\gamma(\text{C}5\text{--C}3\text{--P}1\text{--C}2)$  and  $\gamma(\text{C}4\text{--C}2\text{--P}1\text{--C}3)$  and  $\gamma(\text{F}11\text{--C}5\text{--C}3\text{--P}1)$  and  $\gamma(\text{F}10\text{--C}4\text{--C}2\text{--P}1)$  were fixed. The position of F12 was described by the  $\alpha(\text{F}12\text{--C}4\text{--F}10)$  angle, and its difference with  $\alpha(\text{F}10\text{--C}4\text{--C}2)$  was fixed. The F13, F14 and F15 atoms were described similarly. The position of the H16 atom was fixed relative to P1. The rms vibrational amplitudes were refined in groups corresponding to distinct peaks on the radial distribution curve.

The model of  $(\text{C}_2\text{F}_5)_2\text{POH}$  was very similar to that of  $(\text{C}_2\text{F}_5)_2\text{PH}$ , described above, with an additional three independent parameters [ $r(\text{O}16\text{--P}1)$ ,  $\alpha(\text{O}16\text{--P}1\text{--C}2)$ ,  $\gamma(\text{O}16\text{--P}1\text{--C}2\text{--C}3)$ ] describing the oxygen atom. The position of the H17 atom was fixed relative to that of O16. All fixed differences were taken from the O3LYP/aug-cc-pVTZ calculations.

**Supporting Information** (see footnote on the first page of this article): Calculated relative energies and abundances for conformers of  $(\text{C}_2\text{F}_5)_2\text{PH}$  and  $(\text{C}_2\text{F}_5)_2\text{POH}$ ; potential energy surface for B conformers of  $(\text{C}_2\text{F}_5)_2\text{POH}$ ; experimental and theoretical geometrical parameters of  $(\text{C}_2\text{F}_5)_2\text{PH}$ ; total and molecular electron diffraction intensities of  $(\text{C}_2\text{F}_5)_2\text{PH}$  and  $(\text{C}_2\text{F}_5)_2\text{POH}$ ; anharmonic vibrational corrections for  $(\text{C}_2\text{F}_5)_2\text{PH}$ ; experimental and theoretical Cartesian coordinates of  $(\text{C}_2\text{F}_5)_2\text{PH}$  and  $(\text{C}_2\text{F}_5)_2\text{POH}$ .

## Acknowledgments

The authors are grateful to the German Academic Exchange Service (DAAD) for funding a visit of A. V. Z. to Bielefeld University and to the Humboldt Foundation for a stipend for Yu. V. V. This work is part of a Russian–German Cooperation Project (supported by the Russian Foundation for Basic Research, grant number 12-03-91333-NNIO\_a, and the Deutsche Forschungsgemeinschaft (DFG), OB28/22-1). Support by the Deutsche Forschungsgemeinschaft through the program Core Facilities for GED@BI is gratefully acknowledged. Merck KGaA, Darmstadt, Germany is acknowledged for financial support. The authors thank Dr. N. Ignatiev (Merck KGaA) for helpful discussions.

- [1] a) S. Lou, G. C. Fu, *Adv. Synth. Catal.* **2010**, *352*, 2081; b) A. F. Littke, G. C. Fu, *Angew. Chem.* **1998**, *110*, 3586; *Angew. Chem. Int. Ed.* **1998**, *37*, 3387; c) A. F. Littke, G. C. Fu, *Angew. Chem.* **1999**, *111*, 2568; *Angew. Chem. Int. Ed.* **1999**, *38*, 2411; d) A. F. Littke, C. Dai, G. C. Fu, *J. Am. Chem. Soc.* **2000**, *122*, 4020; e) A. F. Littke, G. C. Fu, *J. Org. Chem.* **1999**, *64*, 10; f) J. Kingston, J. Verkade, *J. Org. Chem.* **2007**, *72*, 2816.
- [2] W. Mahler, *Inorg. Chem.* **1979**, *18*, 352.
- [3] S. A. Hayes, R. J. F. Berger, B. Neumann, N. W. Mitzel, J. Bader, B. Hoge, *Dalton Trans.* **2010**, *39*, 5630.
- [4] S. A. Hayes, R. J. F. Berger, N. W. Mitzel, J. Bader, B. Hoge, *Chem. Eur. J.* **2011**, *17*, 3968.
- [5] S. Basu, N. Arulsamy, D. M. Roddick, *Organometallics* **2008**, *27*, 3659.
- [6] M. Ernst, D. M. Roddick, *Inorg. Chem.* **1989**, *28*, 1624.
- [7] R. D. Chambers, *Fluorine in Organic Chemistry*, Wiley, New York, **1973**, p. 345.

- [8] a) M. Henrich, A. Marhold, A. Kolomeitsev, A. Kadyrov, G.-V. Rösenthaller, J. Barten (Bayer AG, Leverkusen), EP1266902, **2002** (*SciFinder Scholar* **2002**:963725); b) M. H. Königsmann, Ph. D. Thesis, University of Bremen, Germany, **2004**.
- [9] N. E. Shevchenko, V. G. Nenajdenko, G.-V. Rösenthaller, *J. Fluorine Chem.* **2008**, *129*, 390.
- [10] M. B. Murphy-Jolly, L. C. Lewis, A. J. M. Caffyn, *Chem. Commun.* **2005**, 4479.
- [11] a) F. W. Bennett, H. J. Emeléus, R. N. Haszeldine, *J. Chem. Soc.* **1953**, 1565; b) H. J. Emeléus, J. D. Smith, *J. Chem. Soc.* **1959**, 375; c) A. H. Cowley, T. A. Furtch, D. S. Dierdorf, *J. Chem. Soc. C* **1970**, 523.
- [12] H. G. Ang, M. E. Redwood, B. O. West, *Aust. J. Chem.* **1972**, *25*, 493.
- [13] a) B. Hoge, J. Bader, B. Kurscheid, N. Ignatiev, E. Aust (Merck, Darmstadt, Germany), WO 2010/009818, **2010** (*SciFinder Scholar* **2010**:111024); b) B. Hoge, J. Bader, H. Beckers, Y. S. Kim, R. Eujen, H. Willner, N. Ignatiev, *Chem. Eur. J.* **2009**, *15*, 3567; c) J. Bader, R. J. F. Berger, H.-G. Stammer, N. W. Mitzel, B. Hoge, *Chem. Eur. J.* **2011**, *17*, 13420; d) B. Kurscheid, L. Belkoura, B. Hoge, *Organometallics* **2012**, *31*, 1329.
- [14] U. Welz-Biermann, N. Ignatyev, M. Weiden, M. Schmidt, U. Heider, A. Miller, H. Willner, P. Sartori (Merck, Darmstadt, Germany), WO 03/087113, **2003** (*SciFinder Scholar* **2003**:837099).
- [15] B. Hoge, P. Garcia, H. Willner, H. Oberhammer, *Chem. Eur. J.* **2006**, *12*, 3567.
- [16] A. Kolomeitsev, M. Görg, U. Dieckbreder, E. Lork, G.-V. Rösenthaller, *Phosphorus Sulfur Silicon Relat. Elem.* **1996**, *109–110*, 597.
- [17] M. F. Ernst, D. M. Roddick, *Inorg. Chem.* **1989**, *28*, 1624.
- [18] T. Mahmood, J. M. Shreeve, *Inorg. Chem.* **1986**, *25*, 3128.
- [19] A. B. Burg, G. Brendel, *J. Am. Chem. Soc.* **1958**, *80*, 3198.
- [20] B. Hoge, C. Thösen, I. Pantenburg, *Inorg. Chem.* **2001**, *40*, 3084.
- [21] Y. Morino, *Acta Crystallogr.* **1960**, *13*, 1107.
- [22] Y. Morino, J. Nakamura, P. W. Moore, *J. Chem. Phys.* **1962**, *36*, 1050.
- [23] L. Hedberg, I. M. Mills, *J. Mol. Spectrosc.* **1993**, *160*, 117.
- [24] L. Hedberg, I. M. Mills, *J. Mol. Spectrosc.* **2000**, *203*, 82.
- [25] V. A. Sipachev, *THEOCHEM* **1985**, *22*, 143.
- [26] V. A. Sipachev, in: *Advances in Molecular Structure Research* (Ed.: I. Hargittai), JAI, Greenwich, **1999**, vol. 5, p. 323.
- [27] V. A. Sipachev, *Struct. Chem.* **2000**, *11*, 167.
- [28] V. A. Sipachev, *J. Mol. Struct.* **2001**, *67*, 567.
- [29] D. A. Wann, A. V. Zakharov, A. M. Reilly, P. D. McCaffrey, D. W. H. Rankin, *J. Phys. Chem. A* **2009**, *113*, 9511.
- [30] D. A. Wann, R. J. Less, F. Rataboul, P. D. McCaffrey, A. M. Reilly, H. E. Robertson, P. D. Lickiss, D. W. H. Rankin, *Organometallics* **2008**, *27*, 4183.
- [31] a) V. A. Sipachev, *J. Mol. Struct.* **1985**, *121*, 143; b) V. A. Sipachev, *Struct. Chem.* **2000**, *11*, 167; c) V. A. Sipachev, *J. Mol. Struct.* **2001**, *67*, 567.
- [32] A. V. Zakharov, S. A. Shlykov, E. A. Danilova, A. V. Krasnov, M. K. Islyaikin, G. V. Girichev, *Phys. Chem. Chem. Phys.* **2009**, *11*, 8570.
- [33] SHELX-97: G. M. Sheldrick, *Acta Crystallogr., Sect. A* **2008**, *64*, 112.
- [34] a) W. J. Hehre, R. Ditchfield, J. A. Pople, *J. Chem. Phys.* **1972**, *56*, 2257; b) M. M. Francl, W. J. Pietro, W. J. Hehre, J. S. Binkley, M. S. Gordon, D. J. DeFrees, J. A. Pople, *J. Chem. Phys.* **1982**, *77*, 3654.
- [35] a) T. H. Dunning Jr., *J. Chem. Phys.* **1989**, *90*, 1007; b) D. E. Woon, T. H. Dunning Jr., *J. Chem. Phys.* **1993**, *98*, 1358.
- [36] A. A. Granovsky, *Firefly*, v. 7.1.G; <http://classic.chem.msu.su/gran/firefly/index.html>.
- [37] M. W. Schmidt, K. K. Baldrige, J. A. Boatz, S. T. Elbert, M. S. Gordon, J. H. Jensen, S. Koseki, N. Matsunaga, K. A. Nguyen, S. Su, T. L. Windus, M. Dupuis, J. A. Montgomery, *J. Comput. Chem.* **1993**, *14*, 1347.
- [38] M. J. Frisch, G. W. Trucks, H. B. Schlegel, G. E. Scuseria, M. A. Robb, J. R. Cheeseman, J. A. Montgomery Jr., T. Vreven, K. N. Kudin, J. C. Burant, J. M. Millam, S. S. Iyengar, J. Tomasi, V. Barone, B. Mennucci, M. Cossi, G. Scalmani, N. Rega, G. A. Petersson, H. Nakatsuji, M. Hada, M. Ehara, K. Toyota, R. Fukuda, J. Hasegawa, M. Ishida, T. Nakajima, Y. Honda, O. Kitao, H. Nakai, M. Klene, X. Li, J. E. Knox, H. P. Hratchian, J. B. Cross, V. Bakken, C. Adamo, J. Jaramillo, R. Gomperts, R. E. Stratmann, O. Yazyev, A. J. Austin, R. Cammi, C. Pomelli, J. W. Ochterski, P. Y. Ayala, K. Morokuma, G. A. Voth, P. Salvador, J. J. Dannenberg, V. G. Zakrzewski, S. Dapprich, A. D. Daniels, M. C. Strain, O. Farkas, D. K. Malick, A. D. Rabuck, K. Raghavachari, J. B. Foresman, J. V. Ortiz, Q. Cui, A. G. Baboul, S. Clifford, J. Cioslowski, B. B. Stefanov, G. Liu, A. Liashenko, P. Piskorz, I. Komaromi, R. L. Martin, D. J. Fox, T. Keith, M. A. Al-Laham, C. Y. Peng, A. Nanayakkara, M. Challacombe, P. M. W. Gill, B. Johnson, W. Chen, M. W. Wong, C. Gonzalez, J. A. Pople, *Gaussian 03*, rev. E.01, Gaussian, Inc., Wallingford, CT, **2004**.
- [39] *CP2K*, v. 2.2.334 (development version), CP2K developers group, **2011**, <http://cp2k.org>; CP2K is available free of charge on the www: <http://cp2k.berlios.de/>.
- [40] J. Van de Vondele, M. Krack, F. Mohamed, M. Parrinello, T. Chassaing, J. Hutter, *Comput. Phys. Commun.* **2005**, *167*, 103.
- [41] a) S. Goedecker, M. Teter, J. Hutter, *Phys. Rev. B* **1996**, *54*, 1703; b) C. Hartwigsen, S. Goedecker, J. Hutter, *Phys. Rev. B* **1998**, *58*, 3641.
- [42] a) R. J. F. Berger, M. Hoffmann, S. A. Hayes, N. W. Mitzel, *Z. Naturforsch. B* **2009**, *64*, 1259; b) W. Zeil, J. Haase, L. Wegmann, *Z. Instr.* **1966**, *74*, 84.
- [43] a) Yu. V. Vishnevskiy, *UNEX*, v. 1.5, **2011**, <http://unexprog.org>; b) Yu. V. Vishnevskiy, *J. Mol. Struct.* **2007**, *871*, 24.
- [44] A. V. Zakharov, S. A. Shlykov, Yu. A. Zhabanov, G. V. Girichev, *Phys. Chem. Chem. Phys.* **2009**, *11*, 3472.
- [45] A. V. Zakharov, S. L. Masters, D. A. Wann, S. A. Shlykov, G. V. Girichev, S. Arrowsmith, D. B. Cordes, P. D. Lickiss, A. J. P. White, *Dalton Trans.* **2010**, *39*, 6960.

Received: March 17, 2013  
Published Online: May 21, 2013